Applied Energy

Modeling and Analysis of Heat Emissions from Buildings to Ambient Air

--Manuscript Draft--

Manuscript Number:	APEN-D-20-04970R1
Article Type:	Research Paper
Keywords:	Buildings Heat Emission; Building Performance Simulation; urban heat island effect; Urban environment; microclimate; Anthropogenic Heat
Corresponding Author:	Tianzhen Hong, PhD Lawrence Berkeley National Laboratory Berkeley, CA United States
First Author:	Tianzhen Hong, PhD
Order of Authors:	Tianzhen Hong, PhD
	Martina Ferrando
	Xuan Luo
	Francesco Causone, PhD
Abstract:	Heat emissions from buildings is a significant source of anthropogenic heat influencing the urban microclimate; however, they are usually oversimplified in urban climate and microclimate modeling. This study developed a bottom-up physics-based approach to calculate heat emissions from buildings to the ambient air and implemented the approach in EnergyPlus. A simple result verification was conducted by comparing the EnergyPlus simulated results against the spreadsheet calculations. Simulations covering 16 commercial building types, four climates, and two energy efficiency levels were conducted to understand and evaluate the building heat emissions and their temporal patterns as well as three major components: (1) building envelope (convective heat transfer to ambient air), (2) zones (air exfiltration and exhaust air), and (3) HVAC systems (relief air and heat rejection from condensers or cooling towers). The main findings are: (1) heat emissions are usually higher than the site energy use (about 2.5 times), and their dynamics should be considered; (2) building characteristics and their energy systems lead to differences in heat emission contributions from the three components, and their dynamics, for example, in the warehouse models, the envelope component accounts for 90.4%, while it is 12.7% for the large office models; (3) for most building typologies, the climate has a strong impact on heat emissions, for example, buildings with dominant heat emissions from the zone exhaust air and/or the HVAC reject heat, a general decrease in heat emissions in hotter climates is observed, while envelope-dominated buildings show the opposite; and (4) building technologies that reduce energy use in buildings may perform differently in reducing heat emissions. The developed heat emissions calculation method can be adopted in EnergyPlus and most other building energy modeling programs. It can provide dynamic building heat emissions as an input to urban climate computational fluid dynamics (CFD) models at a higher spatial and temporal resolution than is currently available, to improve the simulation accuracy of the urban microclimate and capture the urban heat island effect and urban overheating.

Modeling and Analysis of Heat Emissions from Buildings to Ambient Air

Tianzhen Hong[1*], Martina Ferrando[1, 2], Xuan Luo[1], Francesco Causone[2]

[1] Building Technology and Urban Systems Division, Lawrence Berkeley National Laboratory, California, USA

[2] Department of Energy, Politecnico di Milano, via Lambruschini 4, Milan, Italy

*Corresponding author: T. Hong, thong@lbl.gov

Abstract: Heat emissions from buildings is a significant source of anthropogenic heat influencing the urban microclimate; however, they are usually oversimplified in urban climate and microclimate modeling. This study developed a bottom-up physics-based approach to calculate heat emissions from buildings to the ambient air and implemented the approach in EnergyPlus. A simple result verification was conducted by comparing the EnergyPlus simulated results against the spreadsheet calculations. Simulations covering 16 commercial building types, four climates, and two energy efficiency levels were conducted to understand and evaluate the building heat emissions and their temporal patterns as well as three major components: (1) building envelope (convective heat transfer to ambient air), (2) zones (air exfiltration and exhaust air), and (3) HVAC systems (relief air and heat rejection from condensers or cooling towers). The main findings are: (1) heat emissions are usually higher than the site energy use (about 2.5 times), and their dynamics should be considered; (2) building characteristics and their energy systems lead to differences in heat emission contributions from the three components, and their dynamics, for example, in the warehouse models, the envelope component accounts for 90.4%, while it is 12.7% for the large office models; (3) for most building typologies, the climate has a strong impact on heat emissions, for example, buildings with dominant heat emissions from the zone exhaust air and/or the HVAC reject heat, a general decrease in heat emissions in hotter climates is observed, while envelope-dominated buildings show the opposite; and (4) building technologies that reduce energy use in buildings may perform differently in reducing heat emissions. The developed heat emissions calculation method can be adopted in EnergyPlus and most other building energy modeling programs. It can provide dynamic building heat emissions as an input to urban climate computational fluid dynamics (CFD) models at a higher spatial and temporal resolution than is currently available, to improve the simulation accuracy of the urban microclimate and capture the urban heat island effect and urban overheating.

Keywords: Buildings Heat Emission; Building Performance Simulation; Urban Heat Island Effect; Urban Environment; Microclimate; Anthropogenic Heat

1. Introduction

Urban microclimate is affected by morphology and thermal characteristics of the urban environment (e.g., street width, surfaces' solar reflectivity, material roughness, evapotranspiration of surfaces) as well as by anthropogenic heat emissions (e.g., heat releases from buildings, humans, transportation, and industries) [1,2]. In particular, all these features influence the airflow, humidity level, and air temperature of the urban environment [3]. In dense urban areas, the absorption of short-wave radiation from the sun, the increased surface areas capable of storing heat and the resulting anthropogenic heat emissions are boosted [4]. Meanwhile, due to the compactness of the building and street geometry, the long-wave radiative heat loss towards the sky, the evaporation from vegetation and water bodies, and the turbulent heat transport due to the wind are hindered [5]. Moreover, air pollution and the relative greenhouse effect hampers the re-emission of long-wave radiation towards the urban environment [6]. All these factors contribute to the urban heat island (UHI) effect, which is the climatic

phenomenon causing higher air temperatures in dense urban areas compared to the surrounding rural open areas [7]. In recent years, UHI became a huge concern in cities [8], stressed by climate change and the increasing risk of heatwaves [9]. The phenomenon is registered in almost all urban areas, regardless of the city size or the climate [10,11]. For example, in the 1,400 square kilometer (km^2) humid subtropical climate city of Nanjing, China (Köppen climate classification Cfa [12]), the UHI is indicated as a nocturnal phenomenon that can increase the difference in outdoor air temperature between the urban area and its suburbs by 2.2°C [13]. Similarly, in the 260 km^2 continental climate city of Madison, Wisconsin (Köppen climate classification Dfb [12]), in 2012 the registered mean maximum temperature in July was 1.8°C higher than it was in the surrounding rural areas [14]. This substantial increase in temperature affects the energy consumption of buildings [15] and the livability of outdoor areas [16].

Buildings play a fundamental role in the UHI, due to their morphology and surface characteristics. Besides, they count for a large portion of the total anthropogenic heat emission of an urban area. At urban scale, anthropogenic heat emission has four main origins: human metabolism, industry, transport, and buildings [17]. People spend, usually, most of the time inside buildings, but they account for only a small portion of the total latent and sensible heat emissions. For this reason, in several studies, only industry, transport, and buildings are recognized as the main sources of anthropogenic heat [18]. Buildings emit heat to the urban environment to maintain certain indoor temperatures and humidity levels for occupant comfort or process and manufacturing needs. The heat sources of building heat emissions include (1) the received solar radiation on the building's exterior surfaces (walls, roofs) and transmitted through glazing; (2) convective heat transfer between building envelope and ambient air due to temperature difference, and airflow through openings and cracks in the envelope; (3) internal heat gains from energy consumed in buildings to provide services of lighting, HVAC (heating, ventilation, air-conditioning), plug-in equipment, and domestic hot water, and (4) a relatively small fraction of heat from occupants. Buildings emit heat towards the ambient air as sensible and latent heat due to exiting air from the building envelope (e.g., fans, heating and cooling systems, exfiltration, etc.), and as thermal radiation towards the environment (e.g., air, sky, ground, other surfaces) due to differences in surface temperatures. Particularly, in this study, the building heat emission towards the ambient air was considered. Indeed, traditionally in Building Energy Modelling (BEM) the heat emission from buildings is usually not calculated, as it does not directly influence building energy performance. Some specific tools (e.g., Rayman [19], SOLWEIG [20], ENVI-met [21], or CityComfort+ [22]) are usually employed to calculate the effect of buildings on the microclimate. However, in these cases, buildings are simplified as static daily profile of heat sources.

In numerous former studies, the heat emissions from buildings to air is simplified to be equal to their energy consumption [23]. However, recent research confirms that heat emissions from a building could be much greater than its energy use. For example, from the energy simulation of an office building in Houston, Texas (Köppen climate classification Cfa [12]), it emerged that, during summer, the heat emission is between 40% and 70% higher than the energy consumption [24], due to the energy (mainly solar radiation) coming from the environment and the type of cooling system used, such as cooling towers. In recent years, several studies focused on better understanding the relation between heat emissions from buildings and UHI. Numerous studies were conducted to optimize the buildings' geometry to decrease the impact of UHI on new urban areas [4,5,25]. Others are more focused on the modification of the extent of radiative exchange of surfaces (e.g., with green areas [7], cool facades [8], cool roofs [15], or a mixture of these three strategies [26]) or on shifting the heat release in time via buildings' structural heat storage [27] or phase change materials [28].

However, these adaptation techniques only partially consider the anthropogenic heat from buildings because it is not accurately quantified or understood.

Three main approaches are used to quantify building heat emissions: (1) assessment through inventories, (2) assessment through heat energy balances and (3) assessment through building energy models [17]. The inventory approach exploits registered or surveyed energy consumption data to quantify heat emissions from buildings and other sectors in cities [18]. The registered data are directly converted into heat emissions, without considering time delays, heat storage or differentiation between latent and sensible heat. Data are usually spread spatially within the area through different indexes (e.g., district gross domestic product and population density [29], energy statistics related to the building typology [30]). The assessment through inventories approach relies on major assumptions and simplifications, making it easy to implement. Moreover, the needed data are usually available. For these reasons, this method was widely employed in early studies related to anthropogenic heat emission and its impact on urban microclimate [31–33]. However, the main critical problems are the lack of temporal resolution, leading to erroneous temporal distribution, and the assumption that the heat emission from a building is instantly equal to its energy consumption [18]. Besides these weaknesses, this method has been used for numerous studies for cities and large regions (e.g., by Harrison et al. [23] for London, by Klysik [34] for Poland, and by Lee et al. [35] for Korea).

The second approach, assessment through heat energy balances, exploits the idea of defining a control volume containing the urban area under study, and it tracks, via measurements, all the occurring energy inputs and outputs. The energy entering and exiting from the control volume is assessed via measurements and approximations, while the micrometeorological data can be tracked via net radiometers and eddy covariance techniques, for the net radiation and sensible and latent heat fluxes, respectively. The heat emission is then approximated to the difference between the latent and sensible heat fluxes crossing the control volume [18]. This approach, being applied using measurement data, can be used to validate or compare the other methodologies. However, the measurement campaign could be expensive and time-consuming, and it is impossible to split the anthropogenic heat among its sources. This approach was used for numerous city studies (e.g., by Sailor and Hart [36] for 50 cities in the United States and by Hamilton et al. [37] for London). This approach assumes small or no differentiation between the industry/vehicles sector and the building sector. For this reason, numerous researchers started to study this phenomenon by developing the third approach: assessment through building energy models.

The building energy models methodologies are usually bottom-up and try to assess the heat fluxes towards the outdoor environment from different building components [17]. Building energy models are able to assess the building performance for space heating and cooling and ventilation considering internal loads and the environmental boundary conditions. These models are quite accurate in assessing building energy use because they employ largely verified methods with high spatial and temporal resolutions [38]. However, usually, major simplifications are made to allow the representation of the dynamics of loads and the consequent heat emissions from buildings. Actually, the heat emitted from a building as long-wave radiation can hit other surrounding surfaces (e.g., ground, other buildings) which absorb or re-emit eventually, with a time delay, the absorbed heat. Understanding and considering this dynamic is fundamental to assess effective mitigation strategies for heatwaves and UHI [18]. A building emits heat towards the whole surrounding environment (e.g., the air, the sky, the ground,

other buildings, trees, water bodies). In particular, to better study the impact of building heat emission on UHI and microclimate in general, the heat emitted by the buildings towards the ambient air is the predominant topic.

This study aims to develop a novel approach to calculating heat emissions from buildings using a detailed physics-based model, and assess the characteristics and dynamics of building heat emissions across building types, climates, and energy efficiency levels. The outcome of this study provides new insights into the importance and extent of heat emissions from buildings. The study focused on sixteen United States Department of Energy (U.S. DOE) commercial reference building models [39] in four selected typical climate zones with two levels of energy efficiency (corresponding to minimum requirements of ASHRAE Standard 90.1 in 2004 and 2016). These diverse combinations enabled detailed simulation of heat emissions from different building components (e.g., envelope, HVAC systems, exfiltration, cooling towers) and comparative analyses across building types, climates, and energy efficiency levels. The study's outcomes can inform urban planning and mitigation strategies towards UHI, heatwaves, and overall urban overheating due to urban development, climate change, and extreme weather events. Numerous publications exist studying more in detail the heat emission from buildings regarding UHI. The majority of them are focused on the envelope [40,41], and a very limited number are focused on other aspects such as the systems [42] or the ventilation [43]. However, none of the existing methodologies address all the aspects together and with a bottom-up approach. The main novelties of this paper are (1) the use of physics-based equations at a user-defined timestep (implemented in EnergyPlus), (2) the assessment of heat emissions by each individual building component (i.e., envelope, systems and zones), (3) the differentiation between the sensible and latent heat emissions, and (4) the detailed evaluation of heat emisssions across different building typologies, climates and energy efficiency levels.

It is worth noticing that in this study a nomenclature consistent with EnergyPlus was used. Site energy is chosen as the building performance metric in the analyses. Site energy is the sum (converted to have the same energy unit) of all types of fuels (e.g., electricity, natural gas, fuel oil) consumed on-site by a building—that is, the amount of fuel and electricity consumed by a building as reflected in the utility bills. Corresponding to site energy is the source energy, which is the fuel or resources consumed at the power plant, including generation inefficiency and transmission and distribution losses along the energy network (e.g., natural gas pipeline and electric grid).

The remaining of the paper is organized as follows. Section 2 describes the methodology of calculating the heat emissions by three main components (envelope, HVAC, and zones). Section 3 covers verification of the simulated heat emissions. Section 4 describes a case study with results presented in Section 5. Discussion is provided in Section 6, and conclusions are drawn in the last section.

2. Methodology

The proposed methodology relies on a physics-based heat balance model. The model considers the heat emission towards ambient air from three main building components (*Figure 1*): (1) envelope, (2) zones, and (3) HVAC system. Exploiting physics-based heat balance equations, the proposed model provides both spatial and temporal flexibility. Thus, it can be used with any weather dataset and any building model, and it can be exploited at any user-defined time step, from 1 minute to 60 minutes for an annual simulation.

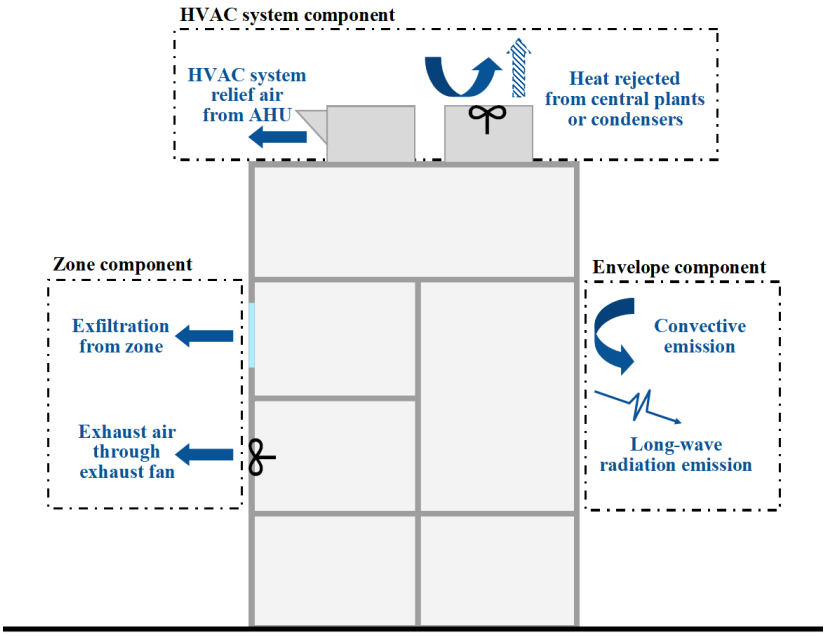

Figure 1: Composition of heat emissions from a building to ambient air

The heat released by the building envelope component includes convection heat to ambient air due to the difference in temperature between the surface temperature and the outdoor air dry-bulb temperature, and the long-wave radiation absorbed by components and particles in the air (i.e., water vapor and pollutants). The zone component includes two types of air discharged from the building: (1) the air exfiltration, i.e., the indoor air which exits without control by openings (e.g., windows, doors) or cracks in the building envelope; and (2) the air exhaust from fans (e.g., in kitchens or bathrooms). Finally, the heat released by the HVAC systems includes the relief air at the air handling units (AHU) and from the possible discharge fuel-gas stacks of gas-fired boilers and furnaces, as well as the heat rejected from (1) air-cooled, evaporative-cooled, and water-cooled condensing units of cooling coils, heating coils, and water heaters; zone HVAC forced air units; evaporative coolers; etc. and (2) plant condensing equipment such as water-cooled chillers. It should be noted that, while the heat emission to ambient air from the envelope is only a sensible load due to the difference in temperatures, the exhaust air through fans, the exfiltration from internal zones, and the HVAC system relief air are all emissions of heat through moist air, and as such, they bring both sensible and latent loads towards the ambient air. The heat rejected by HVAC systems can be only sensible or a mix of sensible and latent emissions, depending on the typology of the system.

The three main components of heat emissions from buildings to ambient air are described in detail in sub-sections 2.1 to 2.3.

2.1. Building envelope component

Considering the heat balance of an exterior surface facing the outdoors the internal and external sources of heat play a fundamental role in the final amount of heat emitted by the building envelope. The solar radiation, outdoor air temperature, internal heat gains, and space cooling/heating influence the temperature of the external surfaces of the envelope. The difference in temperature between the exterior surface and the outdoor air causes heat emissions from the envelope in convective and radiative heat transfer forms).

Note that, in this model, the radiant heat emission towards other surrounding surfaces—including exterior surfaces of nearby buildings, trees, sky, and ground—is not counted, as this portion of the heat is not directly released to the ambient air; whereas, the radiant heat emission towards the air (particles) is included. For this reason, the calculated heat emissions (convective and radiative) are less than the sum of the heat sources. In this case study, the DOE-2 convection model is exploited to calculate the surface outside face convection heat transfer coefficient that is a combination of the MoWiTT and BLAST detailed convection models (equations 3.79 and 3.80 of the Engineering Reference of EnergyPlus are used in this model [44]). While, the linearized radiative heat transfer coefficient calculations follow equation 3.65 in the Engineering Reference [44]. The total heat emissions from the exterior envelope surface ($Q_{emi,surf}$) to the ambient air can be calculated with *Equation 1*. *Figure 2* presents a schematic of the sub-components of heat emissions from building envelope.

$$Q_{emi,surf} = (H_c + H_r) \cdot A \cdot (T_{surf} - T_{out}) \quad [W] \quad (1)$$

where H_c $(W/(m^2K))$ is the surface outside face convection heat transfer coefficient, H_r $(W/(m^2K))$ is the linearized equivalent heat transfer coefficient of the surface (e.g., walls, roofs) outside face thermal radiation to the particles and dust in the ambient air, A (m^2) is the surface area, and T_{surf} (K) and $T_{out}(K)$ are the surface and outdoor air temperature.

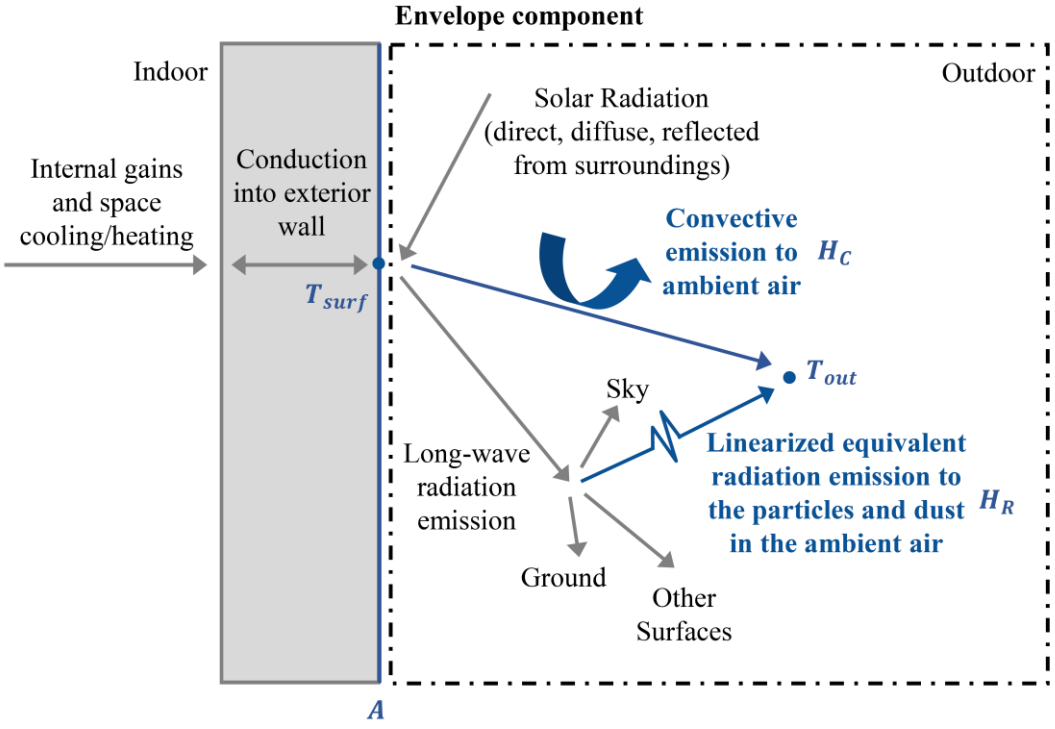

Figure 2: Schematic of the heat emissions from the envelope component

2.2. Zone component

Two general types of heat emissions from the zone component are defined: (1) air exfiltration due to the uncontrolled air flow from the zone to the outdoors through windows, openings, and cracks in the envelope structure; and (2) exhaust air from the zone to the outdoors through exhaust fans or other mechanical equipment. To quantify the sensible and latent heat transported by the exiting air, the differences in the enthalpies of the indoor air of the simulated building zones and the

outdoor air can be exploited. Thus, the total heat released into the ambient air by the exfiltration air from the zones ($Q_{exf,zone}$) and the exhaust air from the zones ($Q_{exh,zone}$) can be calculated with *Equation 2* and *Equation 3*, correspondingly.

$$Q_{exf,zone} = m_{exf} \cdot (h_{zone} - h_{out}) \quad [W] \quad (2)$$

$$Q_{exh,zone} = m_{exh} \cdot (h_{zone} - h_{out}) \quad [W] \quad (3)$$

where m_{exf} ($\frac{g}{s}$) is the exfiltration air mass flow rate, m_{exh} ($\frac{g}{s}$) is the exhaust airflow mass flow rate from the zone, and h_{zone} ($\frac{J}{g}$) and h_{out} ($\frac{J}{g}$) are the zone and outdoor moist air specific enthalpy.

2.3. HVAC system component

The HVAC system component plays a more complex role in the heat emissions of buildings. First, it is involved indirectly in the envelope emission towards the environment by changing the indoor air temperatures via heating and cooling of the zones. Second, the AHU rejects some return air (i.e., relief air) from zones to the outdoors, influencing the heat emissions. Moreover, in the case of boilers and furnaces, it could also reject air towards the environment as waste from the combustion processes. Finally, the HVAC systems reject heat through condensers (located outdoors) for air-cooled systems or cooling towers for water-cooled chilled water systems.

The heat emissions related to the AHU relief air (i.e., the portion of the return air that is exhausted while the other portion gets recirculated to spaces after mixing with outdoor air and being conditioned) can be calculated in a way similar to that of the heat emissions from zones. *Equation 4* can be used to calculate heat emissions by AHU relief air:

$$Q_{AHU} = m_{AHU} \cdot \left(h_{AHU\_out} - h_{out}\right) \quad [W] \quad (4)$$

where m_{AHU} ($\frac{g}{s}$) is the relief air mass flow rate from the AHU and h_{AHU_out} ($\frac{J}{g}$) and h_{out} ($\frac{J}{g}$) are the AHU outlet air and outdoor moist air specific enthalpies.

Conversely, the HVAC system equipment releases heat towards the ambient air also via heat waste for gas-powered combustion units and via condensing units of refrigeration cycles. However, the detailed heat emissions from the HVAC system remain strictly related to the characteristics and the typology of the system. In the case of gas-powered combustion units, the heat emission rate is calculated as the difference between the fuel generated heat (useful energy) and the fuel heat supply. For air-cooled condensing units, it is given by the sum of the cooling rate and the electric power of condenser fan and compressor; and for water-cooled condensing units, it is the total heat transfer rate with outdoor air via cooling towers or evaporative coolers. Further details related to the specific typology of HVAC systems can be found in the Engineering Reference within the documentation of Energy Plus version 9.1 and later [45].

2.4. Implementation in EnergyPlus

The proposed method employs physics-based heat balance equations; thus, it can be implemented in any building energy modeling tool that relies on a similar approach. In this work, as a first implementation, EnergyPlus was chosen. EnergyPlus [46] is a BEM software, allowing the dynamic calculation of numerous energy flows (e.g., space heating and cooling, water, and electric usage, and on-site generation). In recent years, numerous features were added to better model buildings in complex contexts, such as an urban environment [47]. In particular, the focus is on the interaction of the building with surrounding buildings and the local microclimate. Thus, the heat emission calculations were implemented in EnergyPlus as a new feature in version 9.1. The object Output:Table:SummaryReports adds choices of HeatEmissionsSummary and HeatEmissionsReportMonthly to report the annual and monthly heat emissions from the buildings towards the ambient air in tabular summary reports. The heat emissions are grouped as (1) Envelope Convection, (2) Zone Exfiltration, (3) Zone Exhaust Air, (4) HVAC Relief Air, and (5) HVAC Reject Heat. The Envelope Convection includes the convective heat emission from exterior surfaces (e.g., roofs, walls, windows). The Zone Exfiltration and the Zone Exhaust Air components are related to the zone component (i.e., $Q_{exf,zone}$ and $Q_{exh,zone}$). The HVAC Relief Air component includes the AHUs (i.e., Q_{AHU}), and the HVAC Reject Heat component includes the boiler-combustion exhaust, cooling towers, air-cooled condensers, etc. Finally, twelve variables are added to report time-step results, divided into total, sensible, and latent heat emissions. Specifically, they are: Zone, Average, Surface Outside Face Thermal Radiation to Air Heat Transfer Rate [W]; Zone, Average, Surface Outside Face Heat Emission to Air Rate [W]; HVAC, Average, Zone Exfiltration Heat Transfer Rate [W]; HVAC, Average, Zone Exfiltration Sensible Heat Transfer Rate [W]; HVAC, Average, Zone Exfiltration Latent Heat Transfer Rate [W]; HVAC, Average, Zone Exhaust Air Heat Transfer Rate [W]; HVAC, Average, Zone Exhaust Air Sensible Heat Transfer Rate [W]; HVAC, Average, Zone Exhaust Air Latent Heat Transfer Rate [W]; HVAC, Sum, Site Total Zone Exfiltration Heat Loss [J]; HVAC, Sum, Site Total Zone Exhaust Air Heat Loss [J]; HVAC, Sum, HVAC System Total Heat Relief Energy [J]; and HVAC, Sum, HVAC System Total Heat Rejection Energy [J]. It must be noted that positive values of these reports indicate that the building is releasing heat towards the ambient air, while negative values mean that the building absorbs heat from the ambient air.

3. Model Results Verification

In this study we used the U.S. DOE's commercial reference models [39]. These models already have been validated from the energy use perspective, however, the heat emissions from buildings are not covered in the validation process defined in ASHRAE Standard 140 [48]. Thus, a simple results verification approach was here proposed to verify the calculations. EnergyPlus undergoes verification tests before each release to the public [49,50]. For this reason, the individual parameter values used in the heat emission equations can be taken as reliable, and this verification serves as an engineering check only for the newly implemented equations. Therefore, from the simulations, all the hourly variables needed for the implementation of the heat emission calculations were reported. Eventually, the EnergyPlus simulated heat emissions were compared with the calculated results from a spreadsheet implementing those equations to ensure they are within a narrow range of errors.

The building model selected for this verification was Case 600 from the ASHRAE Standard 140 [48]. *Table 1* summarizes the main characteristics of the case model. The original model is helpful to verify the envelope and zone component of the heat emissions. Moreover, an auto-sized packaged terminal heat pump (PTHP) was added to verify the heat emissions from the HVAC system component. *Equation 1* and *Equation 2* were used for the verification of the envelope and zone components. In particular, *Equation 2* was used assuming a fixed Exfiltration Mass Flow Rate of 0.012 kilograms per second (kg/s) (by ignoring the change of air density due to temperature). *Equation 5* can be used to calculate the HVAC heat rejection energy:

$$Q_{HAVC,\ rej} = (\text{PTHP Electric Energy (Heating Mode)} - \text{PTHP Total Heating Rate}) + (\text{PTHP Electric Energy (Cooling Mode)} + \text{PTHP Total Cooling Rate}) \quad (5)$$

Table 1: Main characteristics of Case 600 (for further details, refer to ASHRAE Standard 140 [48]*)*

	Case 600
Weather data	DRYCOLD.TMY (Golden, Colorado [U.S.])
Geometry	48 m^2 floor area, single-story, rectangular-prism, low-mass building with 12 m^2 of south-facing windows
Material Properties	Table 5-1 in Section 5.2 of ASHRAE Standard 140-2017 [48]
Ground Coupling	The exterior surface of the floor is thermally decoupled from the ground with very thick minimum density and specific heat underfloor insulation
Infiltration	0.5 air changes per hour (ach) continuously (24 hours per day for all year)
Internal Heat Gains	The internal gains are only sensible and constant 200 watts (W) (24 hours per day for all year). 60% radiative, 40% convective
Radiative properties and Surface coefficients	Tables 5-3, 5-4, 5-5 in Section 5.2 of ASHRAE Standard 140-2017 [48]
Window properties	Tables 5-6, 5-7 in Section 5.2 of ASHRAE Standard 140-2017 [48]
Mechanical systems (added)	Packaged Terminal Heat Pump

The results of the verification are presented in *Figure 3* and *Figure 4*. In particular, in *Figure 3*, the spreadsheet calculated and EnergyPlus simulated annual heat emissions from the three components are plotted. For the exfiltration heat loss and the HVAC heat rejection heat, an increase of 1% and 5% was observed. Conversely, a slight decrease of 1% was reported for the EnergyPlus simulated surface heat emission. *Figure 4* shows the distribution in terms of hourly values of the spreadsheet calculated and the EnergyPlus simulated, as well as their differences. The general hourly distributions of the calculated and simulated values were very similar for all three components; also, the error distribution was relatively small. These small differences were caused by the assumption of constant air density in the spreadsheet calculations, as well as the use of different time step in the calculations (the spreadsheet uses an hourly time step while EnergyPlus uses 10-minute time step). Note that the relatively high value of +5% registered for the HVAC heat rejection heat was caused by an unbalanced distribution of the error being always negative (i.e., the spreadsheet calculations underestimate heat emissions from the air-cooled condenser). For the Surface Heat Emission and the Exfiltration Heat Loss, the distributions of the error were larger, but they cancelled out between positive and negative values, leading to a smaller difference in annual values.

In summary, the dynamics and annual sum of the heat emission from the three components (i.e., envelope, zone, and HVAC systems) simulated by EnergyPlus were verified and coherent with the physical approach adopted.

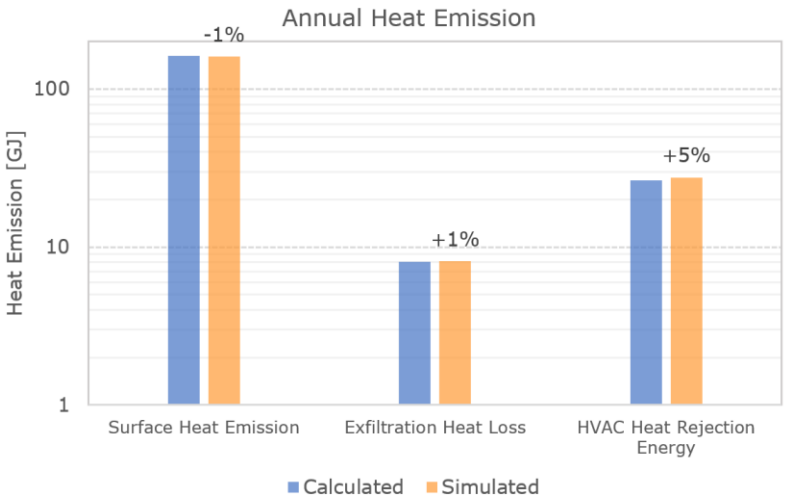

Figure 3: Total Annual calculated and simulated heat emission

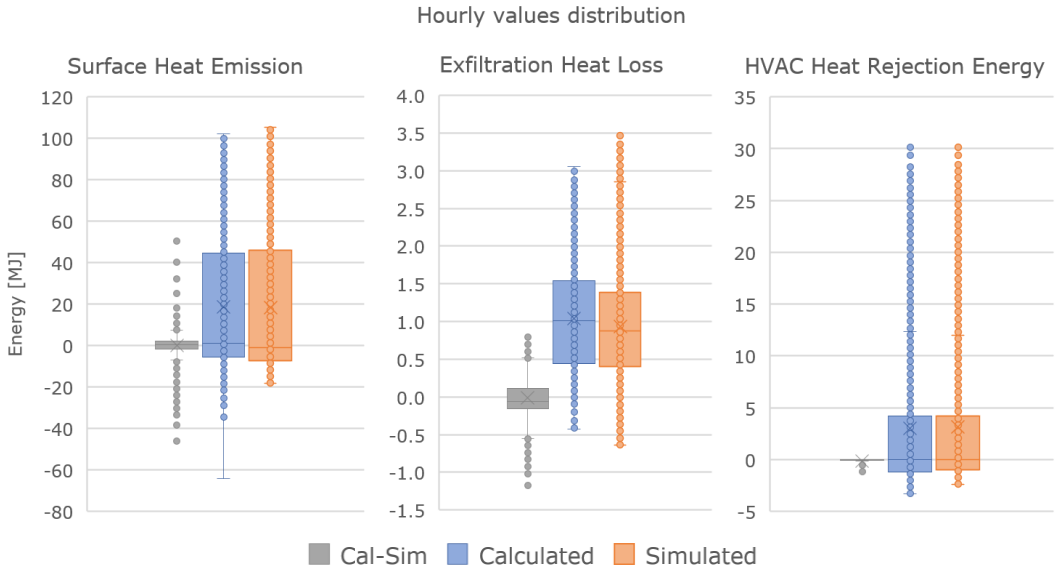

Figure 4: Hourly spreadsheet calculated (in blue) and EnergyPlus simulated (in orange) heat emissions

4. Case Study

The U.S. DOE developed the commercial prototype building models to represent about 70% of the commercial buildings in the United States, and they are popularly used in building simulation as a reliable baseline of comparison [39]. The prototype models include 16 commercial building types characterized for 17 climate locations (across all eight U.S. climate zones) and five different energy efficiency levels in accordance to recent editions of ASHRAE Standard 90.1. In this study, the 16 commercial prototype building models were used to quantify and understand the differences within buildings related to their heat emissions. The 16 building models for the two energy efficiency levels of 2004 and 2016 across four typical climates of Fairbanks, New York, San Francisco, and Tampa were chosen for the study, with a combination of 128 simulations. Table 2 describes the main characteristics of the four chosen locations. The four locations should give a good overview of the differences in U.S. climates, considering their differences in heating degree days (HDD) (i.e., from 7,295 in Fairbanks to 527 in Tampa) and the cooling degree days (CDD) (i.e., from 14 in San Francisco to 1,765 in Tampa). Fairbanks is classified as a subarctic climate (Dfc) in the Köppen climate classification [12]. It is characterized by long, usually very cold winters and short, cool to mild summers proved by the average dry bulb temperature of the weather dataset

(-1.7°C) and a relatively high difference of 35°C between monthly average (given by the difference between a monthly average of -19°C in December and 16°C in July). New York and Tampa are both classified as a humid subtropical climate (Cfa), characterized by warm and humid summers. However, New York has a greater variability during the year, with cold winters. The yearly average dry bulb temperature is almost 10°C less than the Tampa average and shows a greater maximum difference between monthly averages (25°C for New York and 14°C for Tampa). These characteristics are demonstrated by the large differences in the HDD and CDD of the two climates. San Francisco is classified as a Mediterranean warm summer climate (Csb) because of its mild winters and warm summers. The San Francisco weather is characterized by a small variability within the year, with a maximum difference between a monthly averages of 7°C, a yearly average dry bulb temperature of 14.5°C and lower CDD than Fairbanks.

Table 2: Main characteristics of the weather datasets of the four cities chosen

Location	**Fairbanks, Alaska, U.S.**	**New York, New York, U.S.**	**San Francisco, California, U.S.**	**Tampa, Florida, U.S.**
Data Source	TMY3 702610 WMO	TMY3 744860 WMO	TMY3 724940 WMO	TMY3 747880 WMO
Köppen climate classification [12]	Dfc	Cfa	Csb	Cfa
U.S. DOE climate classification [51]	8	4A	3C	2A
Location	64.82° N 147.85° W	40.65° N 73.8° W	37.62° N 122.4° W	27.85° N 82.52° W
Elevation [m]	133	5	2	8
Yearly average dry bulb temperature [°C]	-1.7	12.1	14.5	21.3
Maximum difference between monthly average [°C]	35	25	7	14
HDD [respect to 18.5°C]	7,295	2,749	1,732	527
CDD [respect to 18.5°C]	19	579	14	1,765

5. Results

The 16 U.S. DOE commercial prototype building models that meet the ASHRAE Standard 90.1-2004 and 2016 were run with the four analyzed weather datasets (Table 2). Annual simulations were conducted with a time step of one hour. The hourly results were eventually aggregated to understand annual and monthly trends in the heat emissions for the different combinations of building typology, energy efficiency level, and climate zone (location). In this section, the annual, monthly, and hourly results of the simulation are presented. In the next section, the main findings from the elaboration of the analysis are discussed.

5.1. Annual results

Figure 5 shows a comparison between the annual total site energy and the annual total heat emission by component. The highest values for both the annual site energy and the annual heat emission on the net floor area basis were registered for the two types of restaurants: Quick and Full Service. In particular, the highest values were registered for the Quick Service restaurant in the climate of Fairbanks for the 2004 energy efficiency level with an annual site energy of 10.6 gigajoules per square meter (GJ/m^2) and an annual heat emission of 18.0 GJ/m^2. This was due to the high site energy of cooking and a

large amount of exhaust air from the kitchen, as well as the relatively cool outdoor air in Fairbanks. The lowest annual site energy intensity was reported for the Warehouses for all different climates, ranging from 0.09 GJ/m^2 in San Francisco with the 2016 energy efficiency level to 0.55 GJ/m^2 for the Fairbanks case with the 2004 efficiency level. Finally, the lowest annual heat emissions were, in general, registered for the mid-rise apartment buildings, ranging from 0.81 GJ/m^2 for the 2016 Fairbanks case to the 1.2 GJ/m^2 for the 2004 Tampa model. On average, the building envelope component counts for 50% of the total heat emission. However, large variability was registered between building typologies. For example, in the Large Office models, the average value for the envelope component was 12.7%, while, on average it was 90.4% for the Warehouse models. The exfiltration heat emissions counted for an average of 2.8% of the total heat emission, ranging between 0.15% for the Out Patient Health Care models and 11.2% for the High-Rise Apartment models. A large part (almost 50%) of the heat emission of the Restaurant building typologies was related to the air exhausted through fans in kitchens, while for other building typologies it counted for a small portion, or null for buildings with no exhaust fans. Negative values of HVAC relief air were registered for the hot climate of Tampa where outdoor air temperature can be higher than the released air at room temperature.

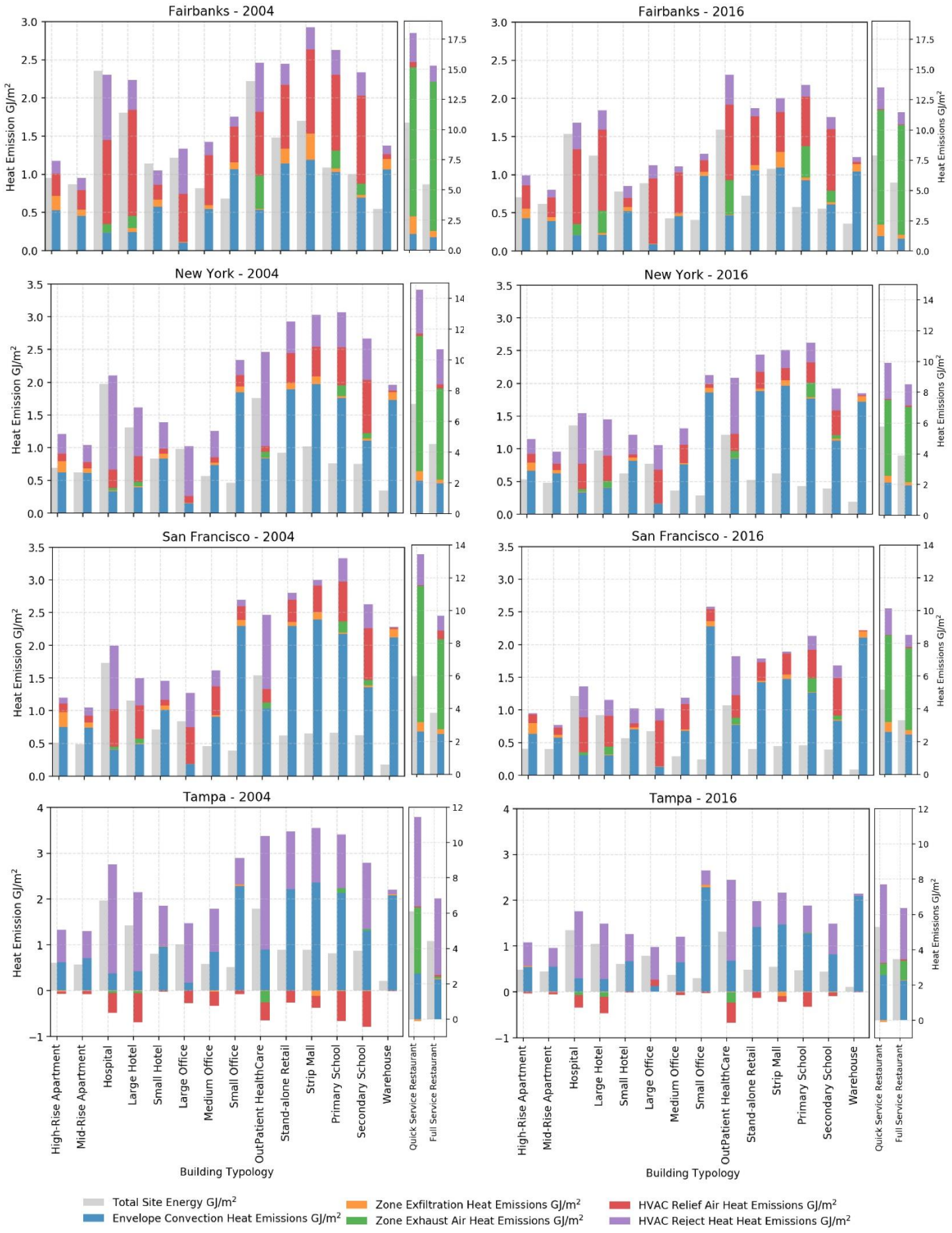

Figure 5: Comparison between the Annual Site Energy and the Annual Heat Emission

Figure 6 presents the ratio between the annual site energy and the annual heat emission. The dotted black line corresponds to ratio = 1. Ratios higher than one were registered in almost all cases. This confirms the strong limitations of approaches in which the heat emission is simplified to be equal to the energy consumption of a building on site. High ratio values were registered in general for Warehouse models, with a peak of 25.2 for the 2016 San Francisco case. The average ratio within all warehouse models was 11.2. Also, in the Small Office models relatively high ratio values were registered, ranging between 2.6 of the 2004 Fairbanks model and 10.7 of the 2016 San Francisco model. Conversely, ratio values around 1 were registered for the Hospital models, ranging between 0.98 of the 2004 Fairbanks model and 1.2 of the 2004 Tampa model. The ratio between the site energy and the heat emission was registered to be lower than 1 in only three cases: Small Hotel and Hospital in Fairbanks, and Large Hotel in Tampa. The ratio averages by building typologies showed that the lowest values were registered for Hospital, Large Hotel, Large Office (i.e., 1.1, 1.3, 1.3 respectively). The highest values were registered for Primary School, Small Office, and Warehouse (i.e., 4.1, 6.2, 11.2, respectively). The Hospital, Large Hotel, and Large Office categories were characterized by the large core floor areas and the largest conditioned building areas (together with the Secondary School). Moreover, Large Hotels and Hospitals were characterized by continuous operation schedules for the HVAC system. For these reasons, the three building typologies were characterized by the highest shares of HVAC reject heat emission due to their systems and relatively high cooling loads. In particular, Hospital and Large Office models were equipped with cooling towers serving the chillers. Consequently, they had relatively high site energy consumption compared to the heat emission, resulting in the ratio being around one. Conversely, Primary School, Small Office, and Warehouse models were characterized by a high envelope emission component due to a higher surface-to-volume ratio, less internal heat gains, and null or almost null exhaust air. Thus, they had a relatively low site energy consumption per building area, resulting in the highest ratios of heat emissions to site energy use.

Comparing different weather datasets, large differences were also registered. The annual heat emissions across different climate zones are organized in *Figure 7*, allowing a direct comparison. When the zone exhaust air and/or the HVAC reject heat played a fundamental role in the total heat emission from the building (e.g., Restaurants, Hospital, Large Hotel, and Large and Medium Offices) a general decreasing trend for hotter climates was registered. However, the opposite trend was recorded for the building typologies in which the total heat emission was envelope-dominated (e.g., Small Office, Warehouse). Indeed, considering the results by component in *Figure 5*, it is evident that the colder the climate, the larger the Zone exhaust and exfiltration air and HVAC relief air heat emission components were; while the hotter the climate, the larger the Envelope component became. Hotter or colder is intended as a general characteristic of the weather dataset, based on their HDD. It is worth notice that the solar radiation for the envelope component, the general condition of the outdoor air, and the CDD play a fundamental role. In fact, these different effects on the single components are why we see quite different behaviors in some New York and San Francisco models (e.g., Stand-alone Retail, Large Office, etc.) in *Figure 7* that do not follow the general trend. For other building typologies (e.g., Apartments, Schools), the differences related to the climate were small. This is because their total heat emission was not driven by a singular component but rather by a mixture of the components affected differently by the climate. Generally, higher relative differences were registered with the 90.1-2016 efficiency level compared to the 2004 one. This is because heat emission decreases greatly for the HVAC-related

components but is relatively constant for components that are generated by an unavoidable difference between the indoor comfort levels (i.e., temperature and humidity) and the external weather conditions.

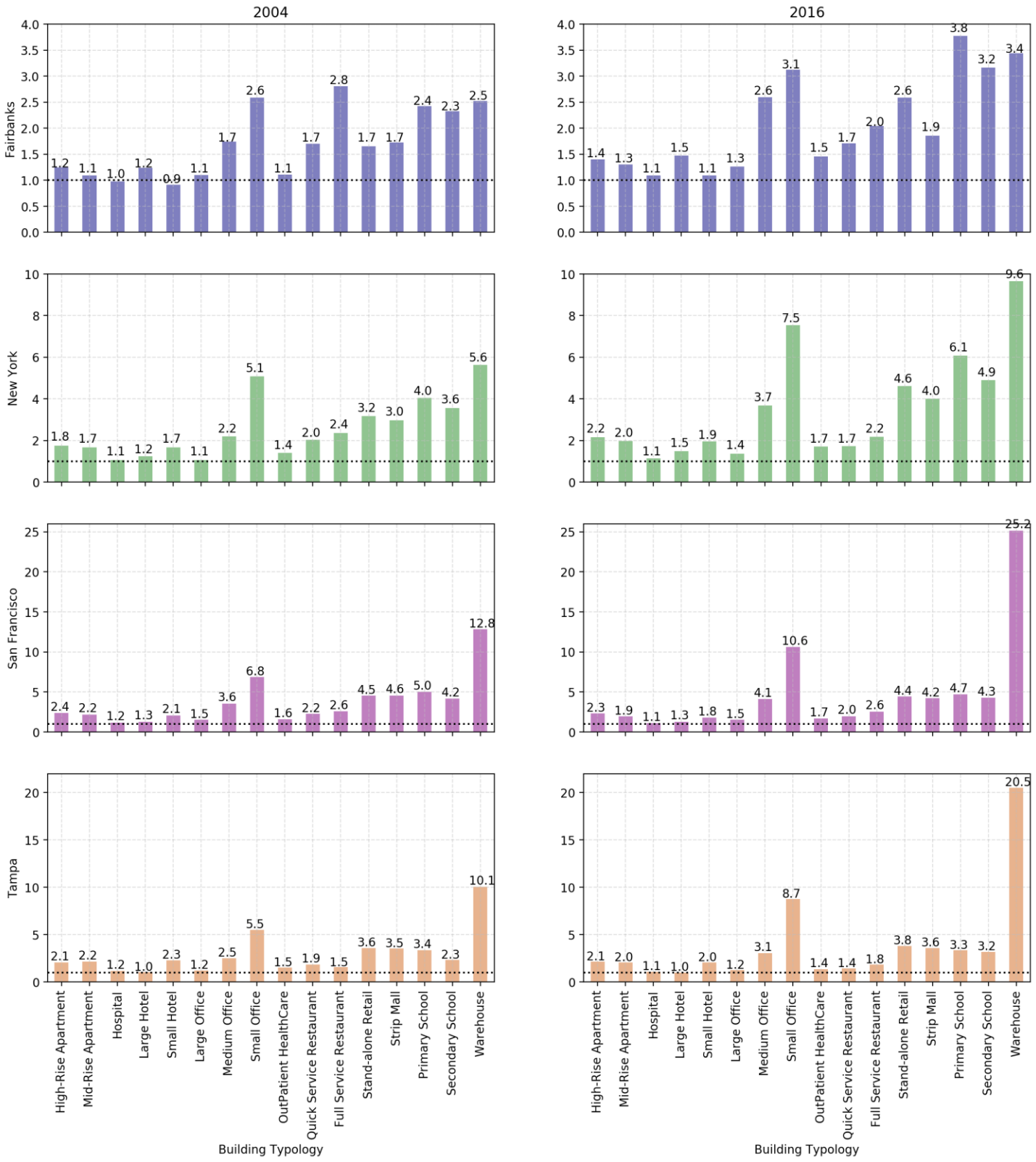

Figure 6: Ratio between the Annual Total Site Energy and the Annual Total Heat Emission (the dotted black line corresponds to ratio = 1)

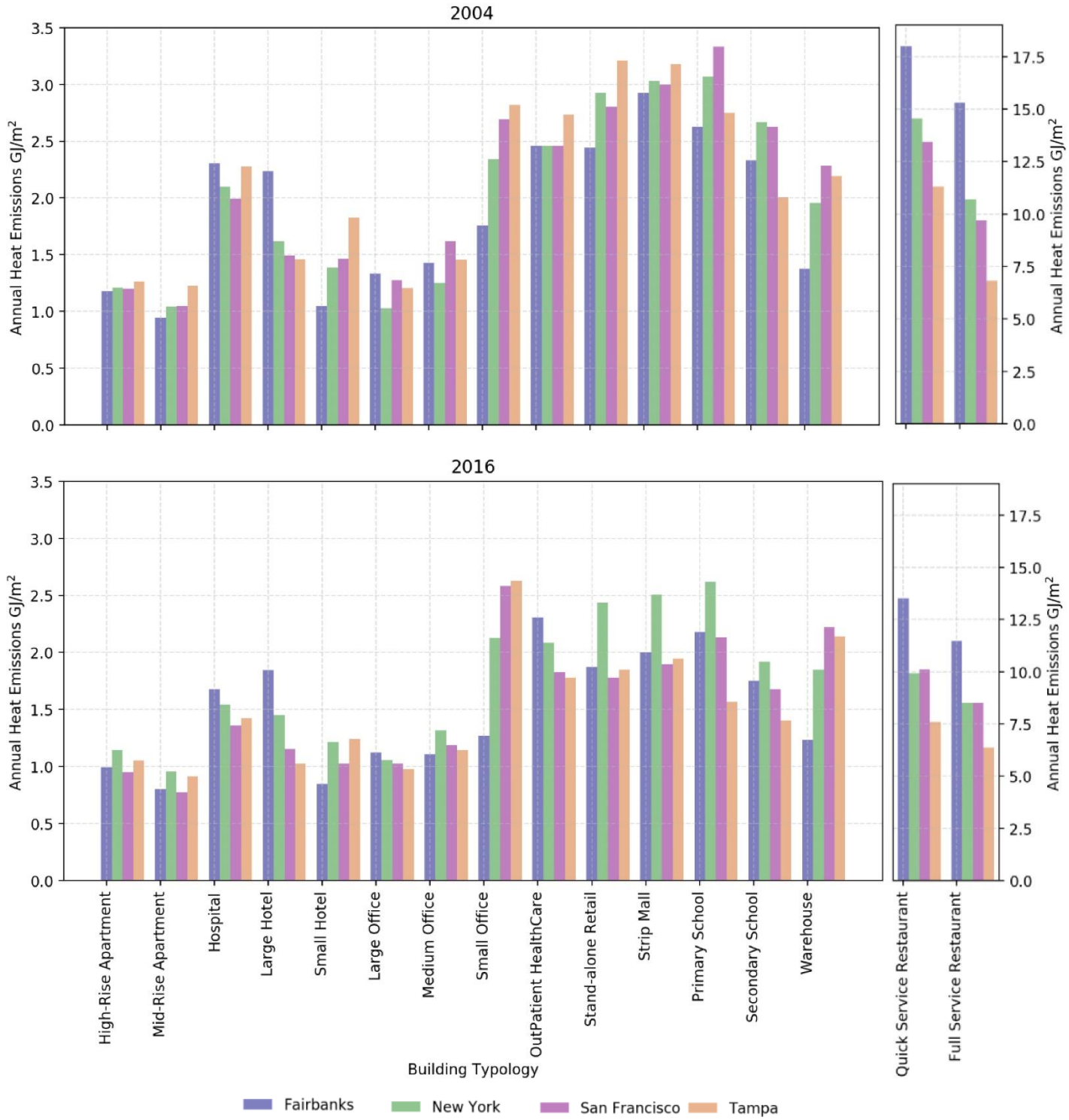

Figure 7: Direct comparison of Annual Heat Emission in different climatic zones

5.2. Monthly results

To better understand the dynamics of the heat emission from buildings. In *figures 8–10*, the monthly heat emissions from the building typologies are reported. In particular, *Figure 8* groups the Residential, Lodging, and Retail models, while

Figure 9 shows the Health Care, Office, and Education building models. Finally, *Figure 10* shows the monthly results for the Restaurant building models, characterized by the highest heat emission per square meter of floor area.

Most building typologies increased their heat emissions during summer, except for the Large Hotel and Restaurants. This corroborates the idea that the higher the solar radiation and/or the outdoor temperature are, the smaller will be the Zone exhaust/exfiltration air and HVAC relief air heat emission components; but the envelope component will be larger. Thus, for most buildings, in which the envelope component is the largest share, the summer corresponds to the peaks in heat emissions. The Large Office model (*Figure 9,* in yellow) was characterized by a quite flat monthly curve; this is because the different components play similar roles in the total heat emission, thus, a balance was reached. Generally, for the building typologies characterized by this trend, the peaks of heat emission are registered around June or July, depending on the climate, for most building typologies. However, the Primary and Secondary school models (respectively in brown and pink in *Figure 9*) are characterized by a net decrease during July and August due to their schedule of occupancy and use. A completely different trend was registered for the Large Hotel (*Figure 8* in green) and Restaurants (*Figure 10*) models. A decrease in monthly total heat emission was registered for the summer months and hotter climates. These buildings, as outlined already with the annual values, were characterized by relatively high HVAC-related heat emission that decreased with the increase of the external temperature. An exception of this trend was registered for the climate of San Francisco, which is characterized by a relatively constant temperature all year long. For the San Francisco models, the heat emission had a winter peak during December and a higher summer peak in June or July.

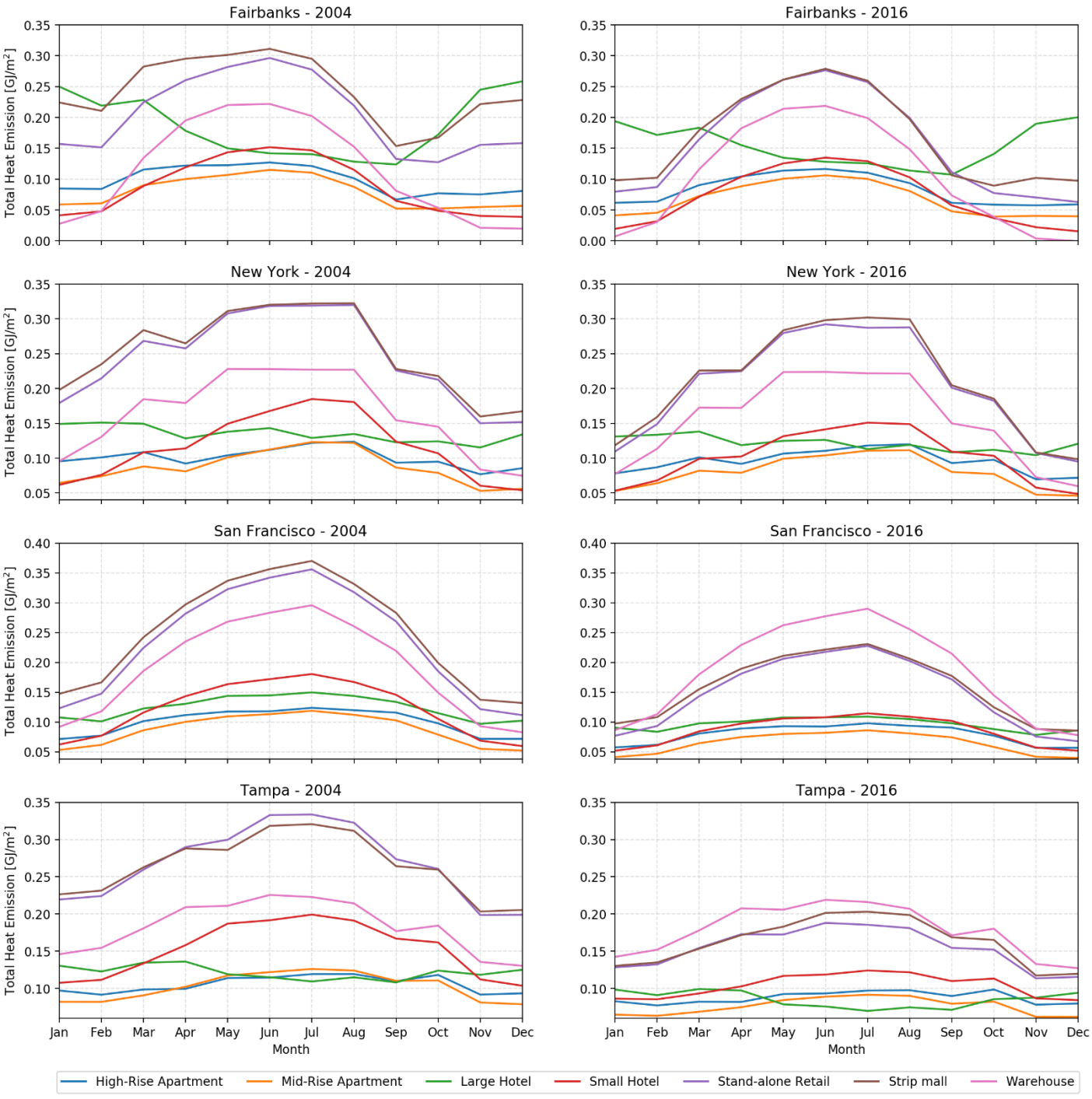

Figure 8: Monthly heat emission results for Residential, Lodging and Retail building function models

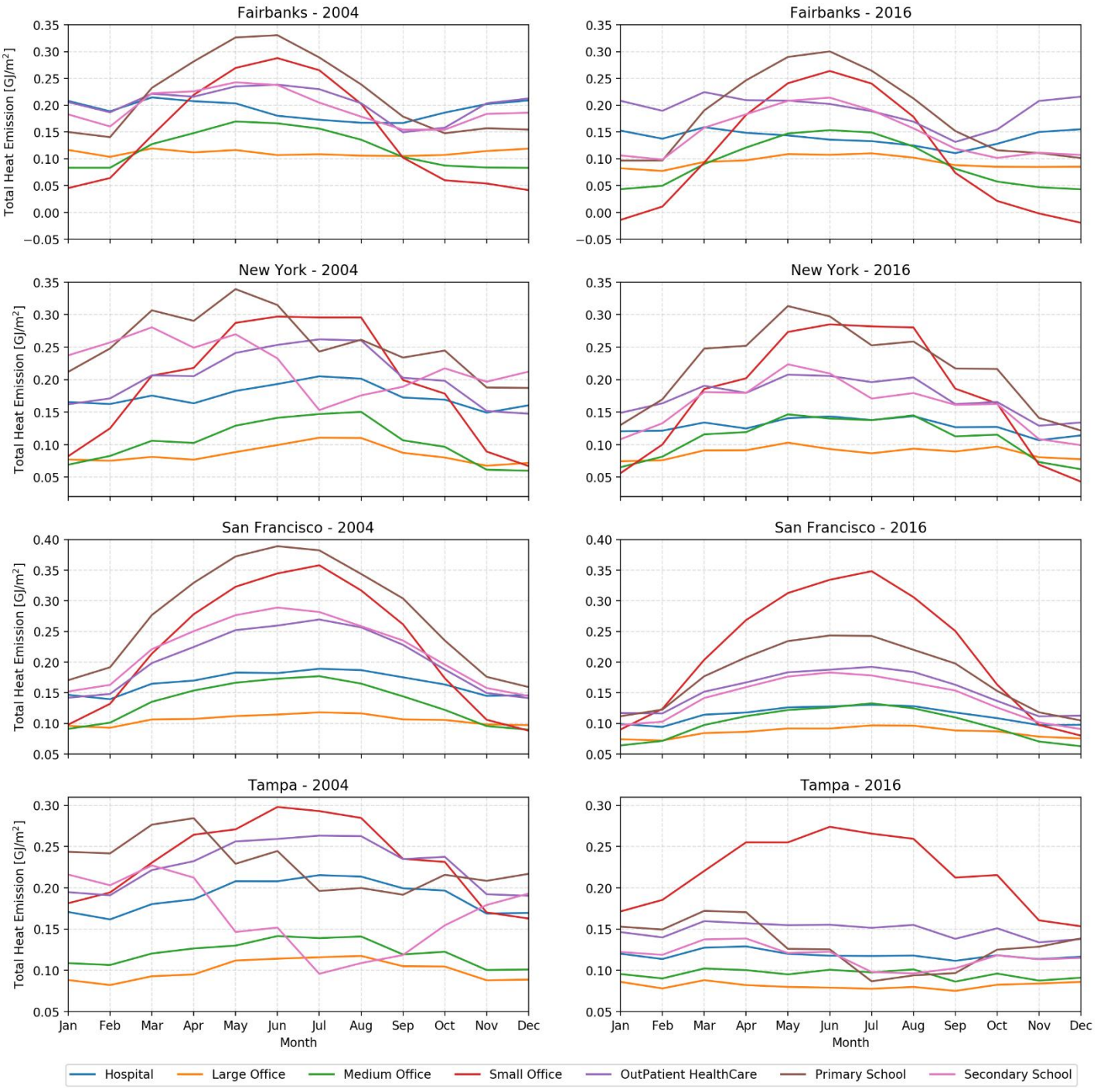

Figure 9: Monthly heat emission results for Health Care, Office, and Education building function models

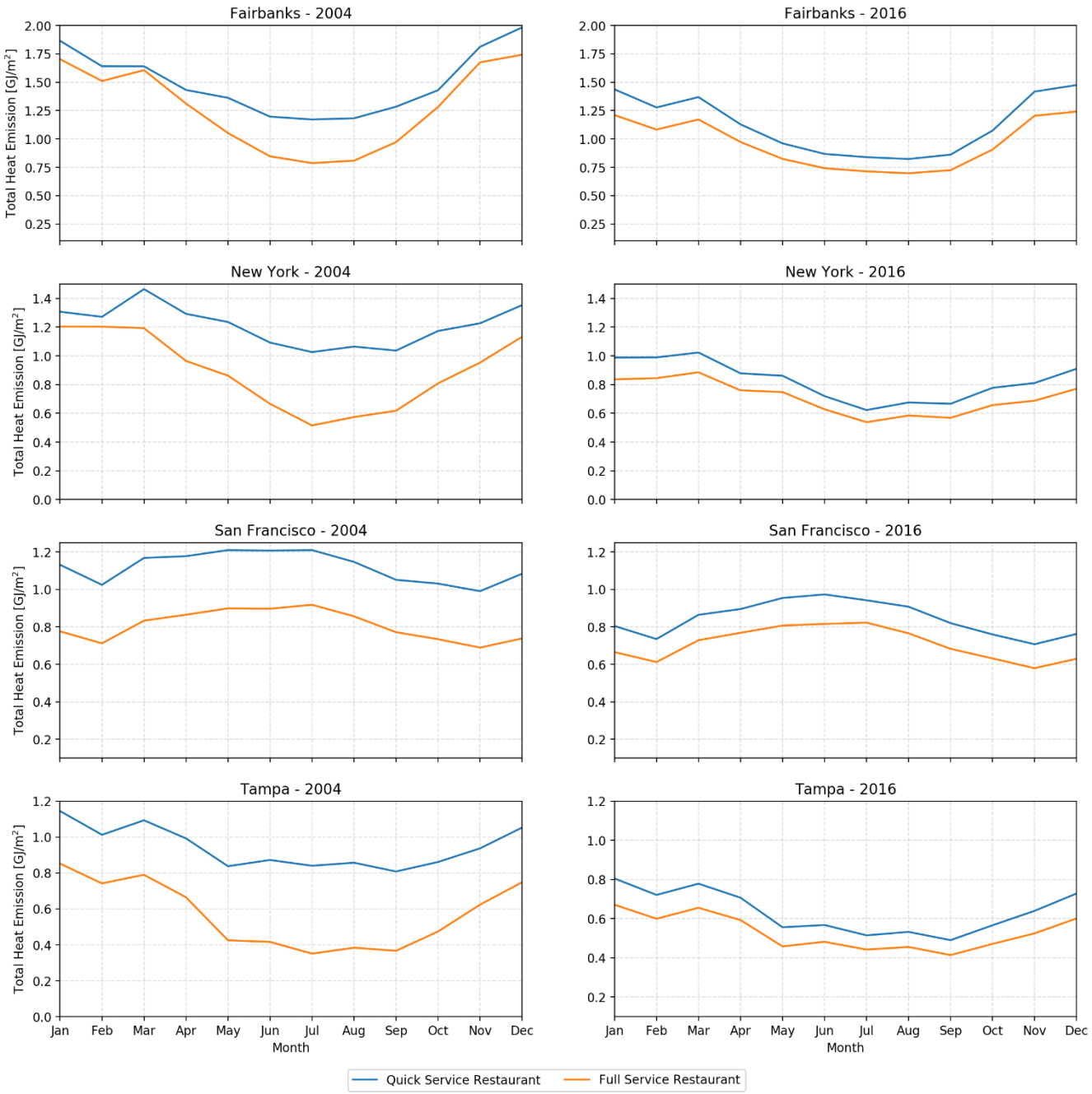

Figure 10: Monthly heat emission results for Restaurants building function models

5.3. Hourly results

In *Figure 11*, the hourly results for four typical weekdays are plotted by components for the Medium Office model; in particular, for the twenty-first of March, June, September, and December. From a comparative analysis with the main weather parameters (i.e., Dry-bulb Temperature, the Global Horizontal Solar Radiation, and the Outdoor Relative Humidity), it is evident that the trend of the envelope component was driven by the solar radiation component. The maximum peaks in the envelope component are usually reached in the same hour of the solar radiation peak. Conversely, the components related to HVAC systems have a trend related to their operation schedule (i.e., between 6 am and 10 pm). When the HVAC systems are on, a correlation with the outdoor air temperature trend can be noticed. Finally, the three peaks registered for the zone exfiltration heat loss correspond to the schedule to model the door openings (with peaks around 8 am, 1 pm, and 6 pm). As the HVAC-related and exfiltration components of heat emissions are highly dependent on the building operation

schedules, their daily patterns differ between occupied (weekdays) and unoccupied days (weekends or holidays). *Figure 12* shows the hourly average heat emission from the different components of the 2016 Primary School model in Fairbanks, divided into weekdays and weekends and holidays. The heat emissions are strictly correlated with the use of the building. Only the envelope component is not as strongly linked with the operating schedules, as a matter of fact, it is more linked to the weather forcing variables.

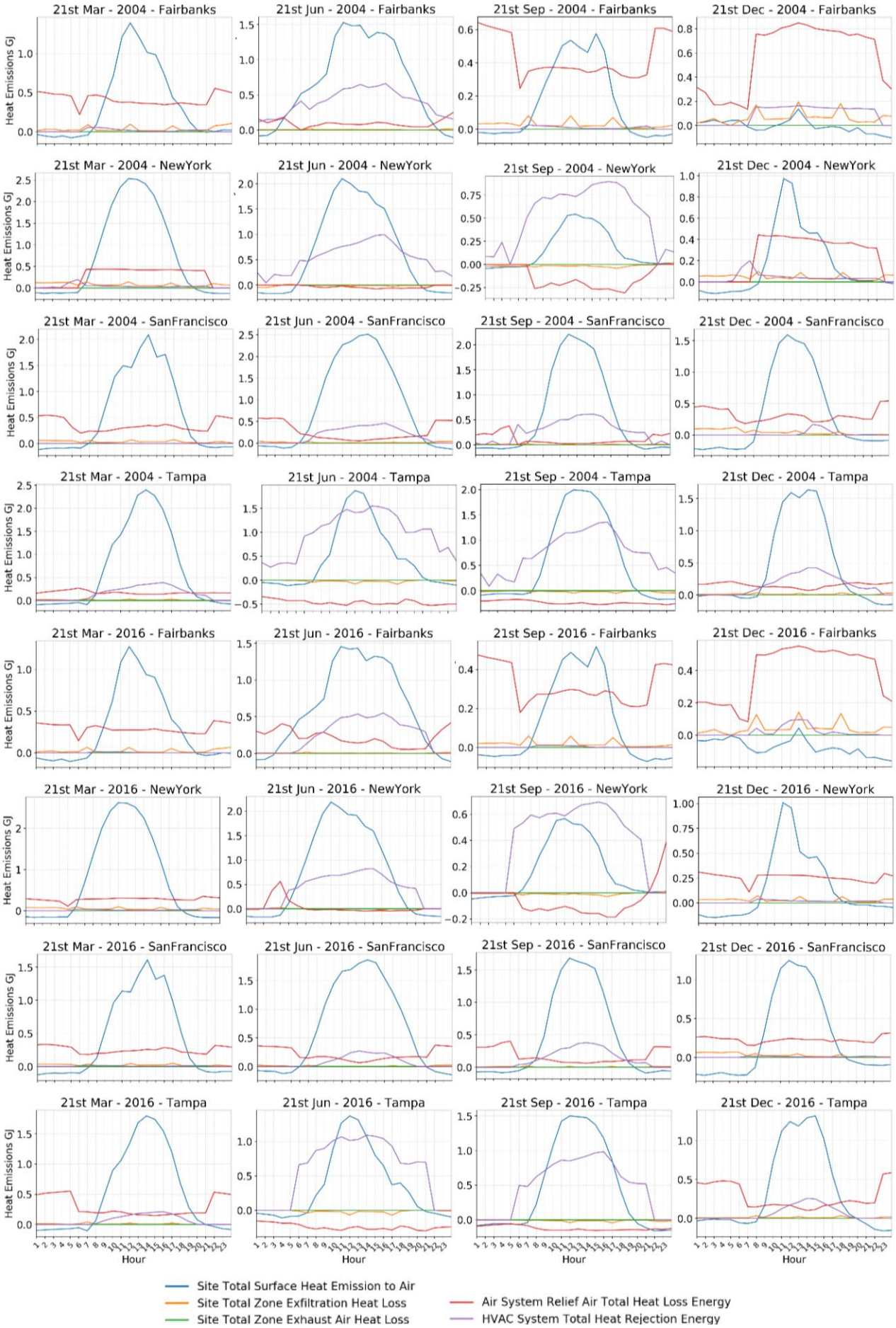

Figure 11: Hourly Heat Emission by component for the 2004 and 2016 Medium Office models

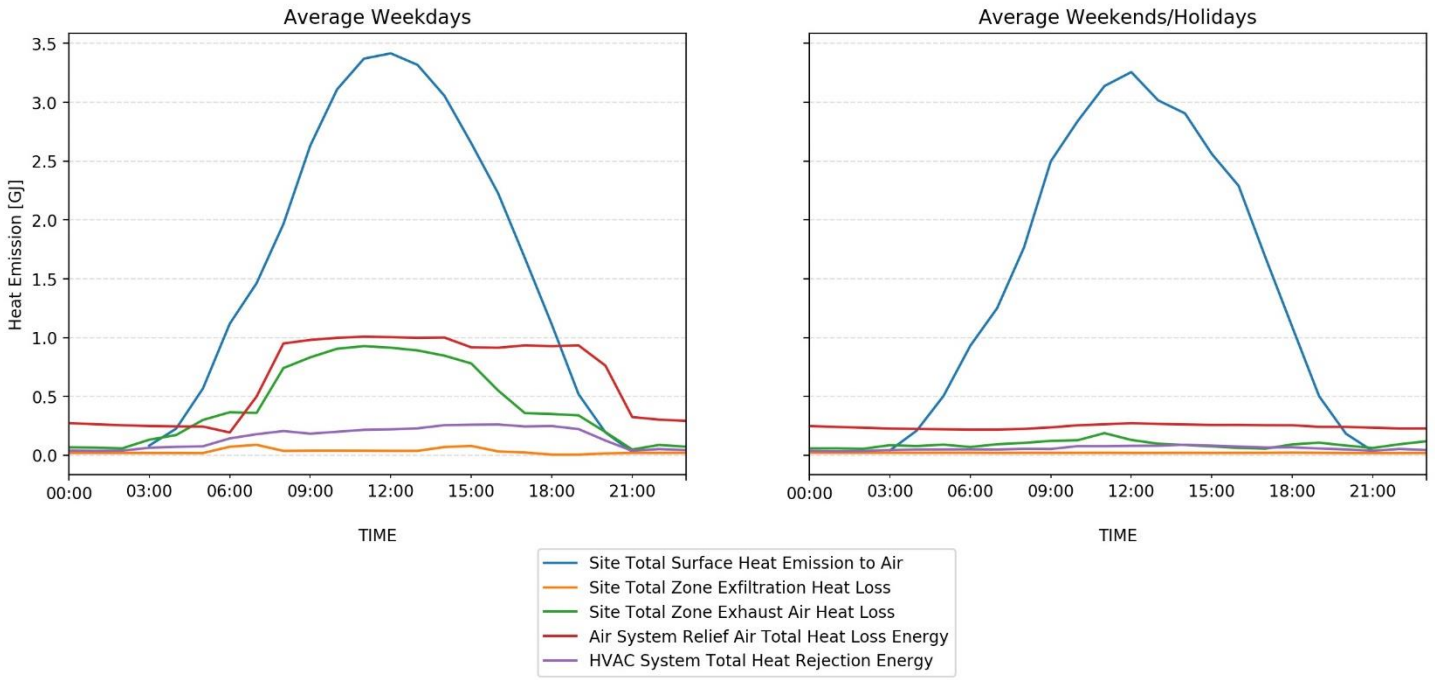

Figure 12: Hourly average divided into weekdays and weekends and holidays for the 2016 Primary School model in Fairbanks

6. Discussion

6.1. Energy savings versus heat emission reduction

Figure 13 reports the ratios between the annual site energy and the annual heat emission of the two energy efficiency levels from ASHRAE 90.1-2004 and 90.1-2016. From the site energy perspective, all the ratios were greater than one. This means that the site energy for the 2004 efficiency level is usually higher than that for 2016. Except for the Fairbanks Full Service Restaurant models, the ratio was slightly lower than one (i.e., 0.98). This is because, in the heating-dominated climate of Fairbanks, the increasing efficiency in the envelope and systems was not able to counterbalance the decrease of internal loads. In particular, the 2016 model showed a strong decrease in the energy used by lighting and electric appliances (e.g., refrigerators), resulting in higher heating energy needs. The heat emission ratios of 2004 models to 2016 models were usually higher than one as well, except for the 2004 New York large and medium office models. This means that in general, a decrease in the site energy use corresponds to a decrease in the heat emissions from buildings. However, the ratios between the heat emissions were mainly lower than those for the site energy, especially in relatively cold climates.

This is caused by several reasons. First, the heat emission is proven to be usually higher than the site energy of a building. Thus, it could be intended as the sum of the site energy of the building and other components (e.g., the heat exchanges between the exterior surface of the envelope and the outdoor air). Second, the general purpose of all the energy conservation measures adopted in the 2016 models had the specific aim to decrease the site energy use rather than heat emissions. Finally, the energy conservation measures had a high impact on the HVAC-related heat emission components, because of the strong increase of the energy efficiency of the building systems. In terms of the envelope, the measures reduce heat emissions on the heat conduction part, however, they are not designed to act on the absorbed and then re-emitted solar radiation. In very few cases (i.e., Large and Medium Office in 2004 New York climate) these measures were worsening the situation (i.e., the

ratio was lower than one). Nevertheless, several exceptions to this trend, with higher values related to heat emission than site energy, were observed for the Restaurant models in the Fairbanks and New York climates, as well as several building types in the San Francisco and Tampa climates. For these climates, a large decrease in the envelope heat emission component was found. Indeed, the relative decrease of envelope heat transfer coefficient (i.e., U-factor) was higher for these two climates than for New York and Fairbanks. Thus, in the future, the energy conservation measures might be improved to also balance UHI.

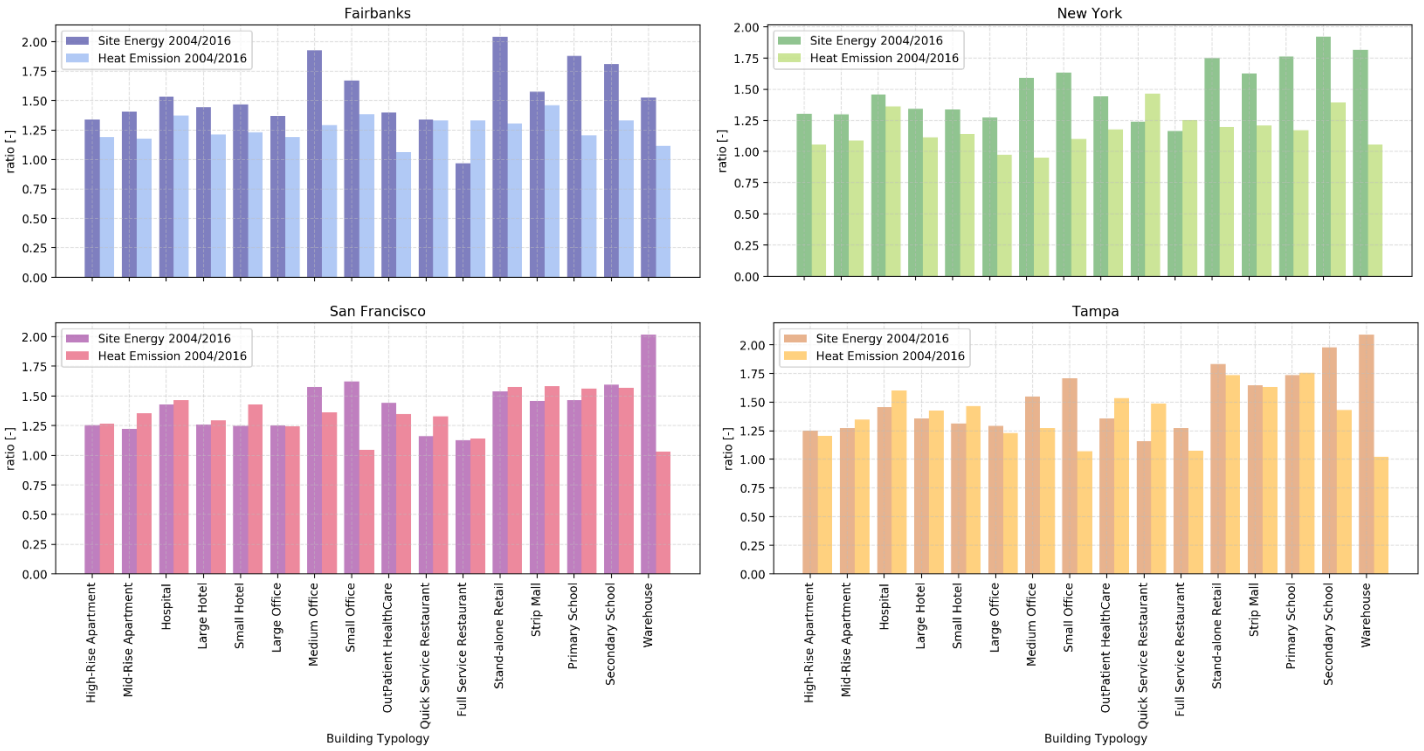

Figure 13: Impact of building energy efficiency levels on the Annual Site Energy and the Annual Heat Emission

6.2. Effect of climate zones

To better understand the effects of climate on the heat emissions, a Pearson correlation analysis was run between the main weather variables (i.e., Dry-bulb Air Temperature, Air Relative Humidity, Air Enthalpy, Horizontal Solar Radiation) and the five heat emission components (i.e., Total Surface Heat Emission to Air, Total Zone Exfiltration Heat Loss, Total Zone Exhaust Air Heat Loss, Air System Relief Air Total Heat Loss Energy, HVAC System Total Heat Rejection Energy) for the 2004 New York Primary School and Hospital model. The Primary School model was chosen because it shows a mixture of all the five heat emission components having a high share of the heat emission related to the envelope. Conversely, the Hospital model is a building in which the heat emission is strongly dominated by the system components. The New York climate was selected because of its high variability of climatic conditions across the seasons.

In *Table 3*, the main findings from the Pearson correlation analysis are presented for the Primary School model. Strong negative correlations were registered between the outdoor air enthalpy and dry-bulb temperature respect to the Total Exfiltration and System Relief Air Heat Losses: -0.86 and -0.83, respectively. Almost perfect negative correlations (i.e., -0.97 and -0.92) were registered between the same weather variables and the System Relied Heat Loss. Moderate positive correlations linked the HVAC System Total Heat Rejection Energy with the same characteristics of the outdoor air:

0.69 and 0.68, respectively. Conversely, an almost perfect positive correlation (i.e., 0.98) was found between the Horizontal solar radiation and the Surface heat emission component. The dry-bulb temperature on this last component showed a weak correlation of 0.35, indicating that solar radiation plays the primary role in heat emission from the building envelope. Table 4 shows the Pearson correlation results for the Hospital model. The general trends of the correlations are quite similar. The relation to the Relative Humidity is similar in absolute values too. Some differences were registered with the Temperature and Enthalpy, as well as the Exhaust and HVAC rejection heat emissions. For these combinations, strong correlations occurred; particularly with the HVAC Heat rejection, the correlations were positive and almost perfect.

Other general trends are outlined from the overall results. In the Fairbanks climate, HVAC relieved heat was prominent due to higher inside and outside enthalpy (or temperature) difference; while San Francisco weather is mild and characterized by strong solar radiation that dominates the surface re-emitting portion. Tampa is cooling intensive, and dominated by HVAC rejections. New York climate, having high HDD and CDD, shows a mixture of these behaviors.

Table 3: Pearson correlation analysis results between output of the 2004 New York Primary School model and the main external weather variables

	Air Dry Bulb Temperature [°C]	Air Relative Humidity [%]	Air Enthalpy [J/kg]
Surface Heat Emission [J]	0.354	-0.372	0.240
Exfiltration Heat Loss [J]	-0.832	-0.252	-0.856
Exhaust Air Heat Loss [J]	-0.078	-0.301	-0.172
Air System Relief Air [J]	-0.920	-0.207	-0.969
Heat Rejection Energy [J]	0.685	-0.063	0.688

Table 4: Pearson correlation analysis results between output of the 2004 New York Hospital model and the main external weather variables

	Air Dry Bulb Temperature [°C]	Air Relative Humidity [%]	Air Enthalpy [J/kg]
Surface Heat Emission [J]	0.333	-0.403	0.217
Exfiltration Heat Loss [J]	-0.852	-0.313	-0.882
Exhaust Air Heat Loss [J]	-0.717	-0.223	-0.769
Air System Relief Air [J]	-0.953	-0.264	-0.997
Heat Rejection Energy [J]	0.901	0.118	0.942

6.3. Effect of building typology

The building typology demonstrates the largest influences in terms of the heat emission absolute quantity, patterns, and intensity. In particular, a sensible spread on the ratio between the site energy use and the heat emission was observed (*Figure 6*). The Small and the Large Office models are an example to better compare two models with the same use function but different characteristics, leading to large differences in their site energy use and heat emission behavior. The Small Hotel model is one of the building typologies in which a large share of the heat emission is from the envelope convective heat transfer to the outdoor air. It is characterized by a small building area with a relatively large surface-to-volume ratio, an average window to wall ratio of 21%, wood-frame walls, and an air-source heat pump providing heating and cooling. Thus, its energy consumption is mainly due to electricity. Conversely, the Large Hotel model is characterized by a large building area, an average window-to-wall ratio of 40%, concrete block walls, a gas-fired boiler for heating, a water source direct

expansion cooling coil, and two water-cooled centrifugal chillers with a cooling tower for cooling. These properties lead to relatively high consumption of natural gas during the winter months and electricity all year long, as well as a high heat emission from the HVAC component. The cooling tower presence is related specifically to the HVAC Reject Heat Emission from the building, as presented in *Figure 14*. Large buildings tend to use central cooling systems with a chilled water plant to meet the intensive cooling loads.

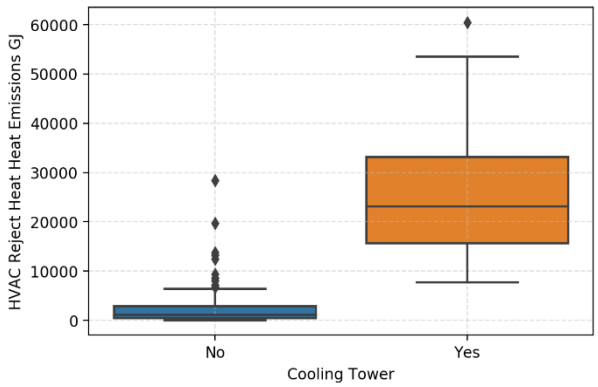

Figure 14: Boxplot relating the HVAC Reject Heat Emission and the presence of a cooling tower in the building

In particular, the heat emission from the Small Office model (*Figure 15*) reaches an evident monthly peak during the summer months, due to the strong correlation between the solar radiation and the surface heat emission that is the largest share of the emission components. Only in the climate of Fairbanks during the winter months did the heat released by the HVAC system exceed the envelope component. The highest peaks for the heat emission from the envelope were reached around June for all climates; while the highest peaks for the HVAC relief heat occurred around July for the climates of Fairbanks, New York, and Tampa. However, the peaks in the San Francisco climate (with the CDD in September) were reached in August for the 2004 model and September for the 2016 model. There is no exhaust fan in the model, so there were no exhaust air-related heat emissions. The exfiltration is also very small due to the tightness of the envelope. For the climates of San Francisco and Tampa, a decreasing trend from the 2004 to 2016 model was observed for all the components.

On the other hand, the heat emission from the Large Office model (*Figure 16*) shows a flatter monthly variation, but the differences were registered between the different components. For example, during the hot summer in New York and the hot weather of Tampa, the HVAC heat rejection reached negative values. For this building typology, there is no exhaust fan and little air exfiltration, so their related heat emission is negligible. The recirculation air is managed almost completely by the HVAC system; hence, the related heat emissions follow the general trend of decreasing during the summer. Again, the envelope component shows similar trends to the other building typologies, with peaks around July for the climates of Fairbanks, New York, and Tampa, and in September for San Francisco. A "compensation" of the heat emission, especially during the hot months, was reported. The summer months registered an increase in the heat emission from the envelope and the HVAC system. At the same time, the summer months affected the heat emission due to the system relief air, with a decrease, being cooler (close to the conditioned room temperature) than the hot ambient air. Thus, the final emissions were relatively low and stayed constant.

Another highlight is that Restaurant models showed a much higher heat emission per building floor area compared to the other building typologies. To better understand the trends and causes of this fact, the monthly site energy use and heat emission by components were plotted for the Quick Service Restaurant in *Figure 17*. The large share of the heat emission from the Quick Service Restaurant models was due to the air exhaust by fans from cooking in the kitchen. The summer months show a decrease of heat emission from the fans, due to the smaller difference in enthalpies between the exhaust air and the outdoor air. Negative values of this component were registered for July in the 2016 New York model and 2004 Tampa model, when the outdoor air was hot; while for the 2016 Tampa model, negative values were reported from May until October. Null or almost null values for the exhaust air component were registered for August for the 2016 New York model and for June and August for the 2004 Tampa model. The zone exfiltration component followed a similar trend. The HVAC heat rejection component had greater monthly variations for the New York and Tampa model, while it remained relatively constant for the Fairbanks and San Francisco models. The results show a larger decrease in the exhaust air heat loss compared to other components between the 2004 and 2016 models. Conversely, the envelope component followed the radiation trend and remained almost constant between the two efficiency levels.

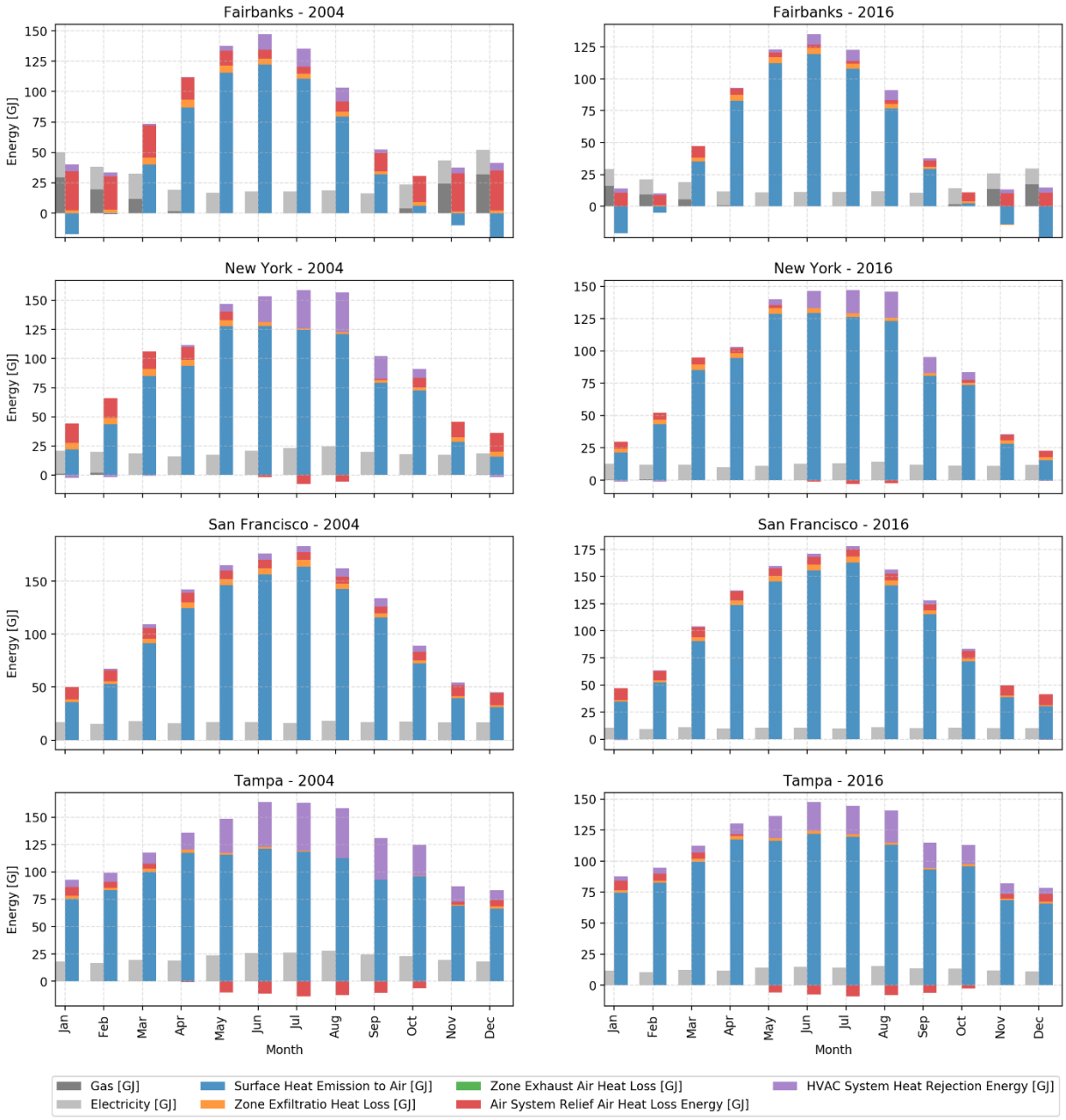

Figure 15: Site energy by sources and Monthly Heat Emission by components for the Small Office models

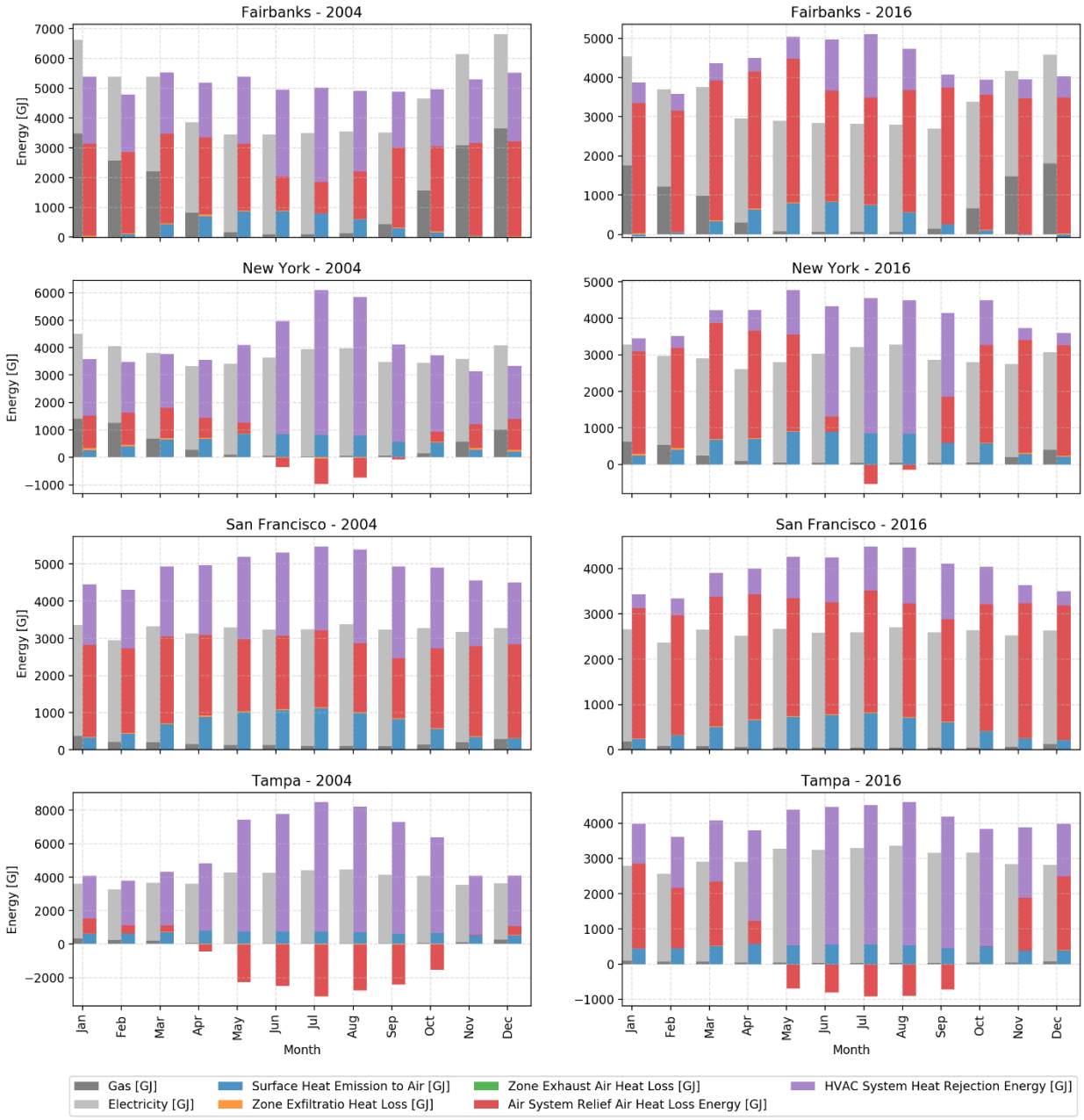

Figure 16: Site energy by sources and Monthly Heat Emission by component for the Large Office models

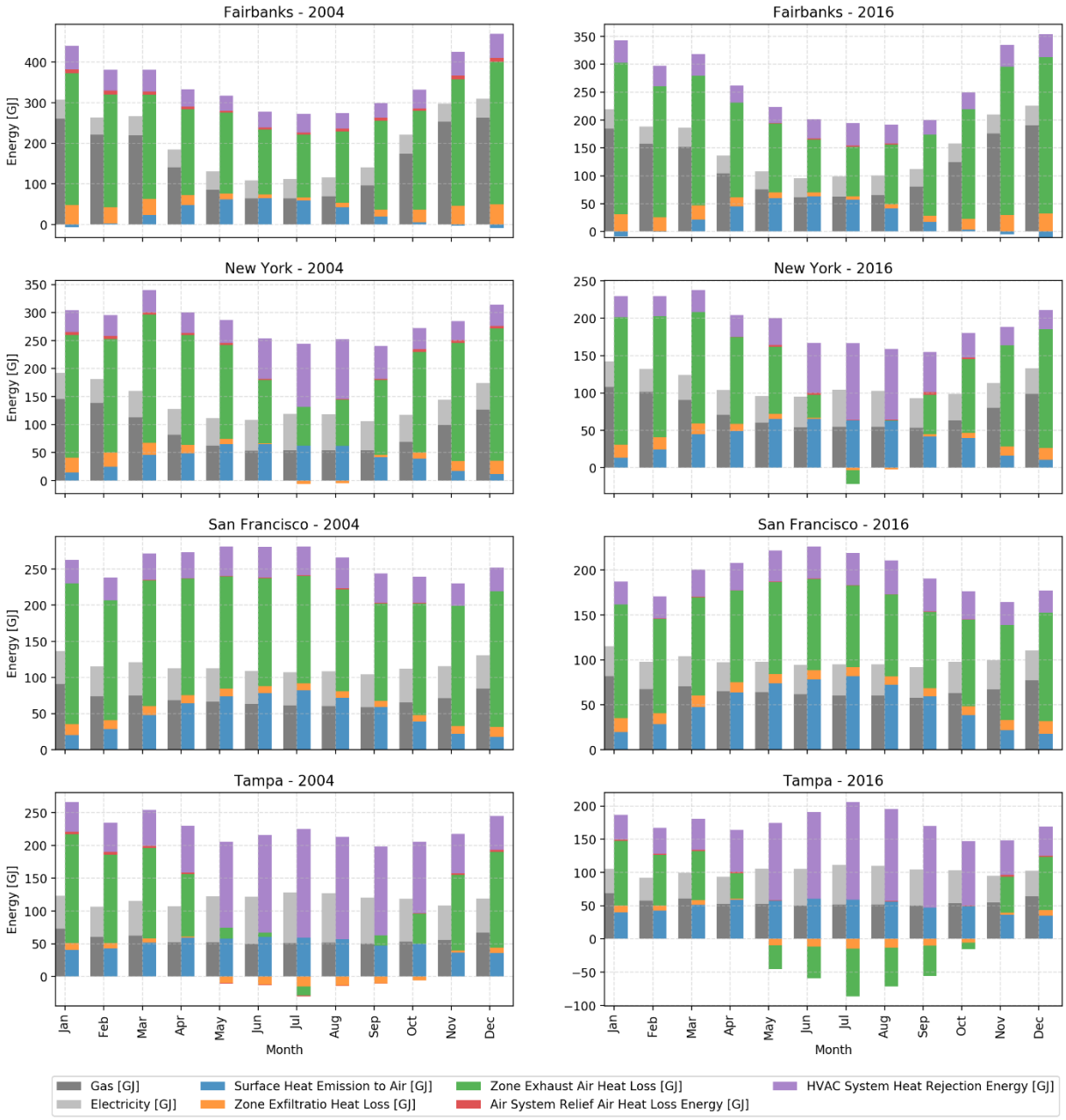

Figure 17: Site energy by sources and Monthly Heat Emission by components for the Quick Service Restaurant models

The building typology characteristics led to a large difference in the ratios between the heat emission and the site energy use. Particularly, the ratio between the Total Site Energy per a building's total air volume is shown in *Figure 18* for the entire set of 128 simulations, i.e., including all the building typologies, climates, and efficiency levels. The building typologies with the lowest total site energy over volume (below 0.08 GJ/m^3) were characterized by different ratios, ranging from about 4 (for the 2016 San Francisco Stand-alone Retail model) to 25 (for the 2016 San Francisco Warehouse model). However, lower ratios corresponded to higher Site Energy use. Moreover, from 0.5 GJ/m^3 and above, an almost flat trend (about 2.5 GJ/m^3) was registered for the ratios. This means that there was not a constant relationship among all building typologies between their site energy consumption and heat emission. However, for high-intensity energy buildings (e.g., Large Hotel, Hospital, Out Patient HealthCare, Full Service Restaurant, Quick Service Restaurant), a clearer relation can be found.

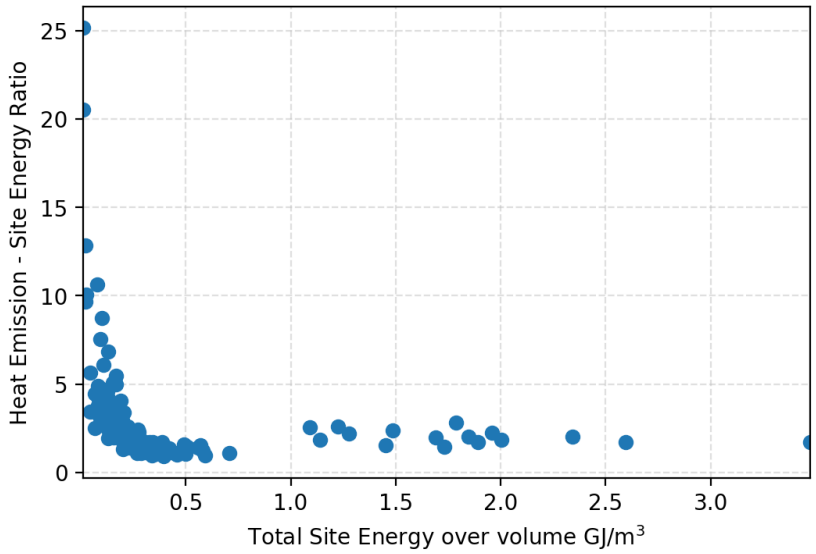

Figure 18: Scatterplot of the Total Site Energy per building air volume and the heat emission-to-site energy ratio

7. Conclusions

This study presents a method to calculate the heat emission towards ambient air from buildings, which can be grouped into three main contributions by components of: (1) building envelope, (2) zones, and (3) HVAC system. The heat released by the envelope component includes exterior surfaces' convective heat to the ambient air and their long-wave radiation towards the moisture and particles in the air including, both in the convection and in the radiation, the solar energy absorbed and re-emitted by walls, roofs, and windows towards the ambient air. The zone component includes two types of air discharged from the building: the exfiltration and the air exhaust by fans. Finally, the heat released by the HVAC system includes the air relief/exhaust by fans in the AHU, as well as heat rejection from cooling towers, air-cooled condensers, and combustion-related exhaust from gas-powered boilers or burners. The HVAC system component of the heat release, during summer cooling mode, is the sum of the building's zone cooling load, the outdoor air conditioning load, and the electricity consumed by the HVAC system to provide the cooling.

A deeper knowledge of the heat release from buildings is fundamental in the understanding and modeling of the microclimate in urban areas, and until now, it has been largely oversimplified. A quantitative assessment of heat emissions from buildings is important to develop effective strategies to mitigate urban overheating and UHI, especially during heatwaves. The method was implemented as a new feature in EnergyPlus version 9.1 using physics-based heat balance equations. A total of 128 building energy models were run, covering 16 U.S. DOE building typologies, four climate zones, and two energy efficiency levels (ASHRAE Standard 90.1-2004 and 2016). In the future, this method could be coupled with a detailed urban microclimate model to better study UHI and its effect on building energy consumption.

To verify the method implemented in EnergyPlus, a simplified spreadsheet calculation was conducted, exploiting the EnergyPlus reported variables used in *Equations 1–5*. The verification model was the Case600 as part of the standard test cases defined in ASHRAE Standard 140, modified with a Packaged Terminal Heat Pump, in the climate of Golden, Colorado (U.S.). The verification results confirmed the validity of the heat emission calculation method.

Simulation results from the 128 building energy models showed that a building's annual site energy use is different from its annual heat emissions. In 70% of the simulations, the heat emissions were higher than their site energy use. However, a great variability was observed; the annual heat emission accounted for from 1 to 25 times the annual site energy use of the building, with an average of about 2.5 times as much. The characteristics of the building and, in particular, its systems, lead to significant differences in the heat emissions by component, as well as the monthly and daily patterns of heat emissions. There are several typologies of buildings (e.g., Warehouse models) for which a large part of the heat emission comes from the envelope component; while for others (e.g., Restaurant models), the main share is related to the exhaust air. The simulation results prove that the heat emission can vary largely by month and by day, thus, its dynamics should not be neglected. The analyses across different climates showed that, for building typologies in which the envelope component has the largest share of the heat emission, the higher the solar radiation, the larger the heat emission from the building, because of the larger temperature difference between the exterior surfaces and the ambient air. Conversely, when the main component is the exhaust air, the heat emission increases for colder climates. However, there are several building types (e.g., Apartments, Malls) that showing a little impact of climate on the heat emission results. In particular, from the hourly analysis of the Medium Office model and the Pearson correlation analysis, it is evident that there is a strong correlation between the envelope component of the heat emission and the solar radiation. The components related to the HVAC system are strongly affected by their operation schedules, equipment efficiency, and the outdoor air temperature.

Limitations of the proposed method include the lack of modeling long-wave radiation between a building and surrounding buildings, which can influence a building's exterior surface temperatures and cooling/heating demand thus heat emissions to the ambient air. Moreover, the building simulations use a preselected annual hourly weatehr file which does not explicitly consider the influence of the heat emissions from the building. Other potentail limitations relate to the algorithms used in EnergyPlus, e.g., the linearization and simplification of some complex physical phenomena in the heat and mass transfer.

Future research can include an integration of the heat emissions from buildings with urban microclimate models (e.g., WRF [52] and CityFFD [53]) via computational fluid dynamics. This is a mandatory step to better understand the urban dynamics in terms of heat exchanges in urban environments. Further insights are also needed on which energy conservation measures usually applied to buildings could be beneficial in reducing heat emissions from buildings, which raises a significant question on how a building design will differ if its performance is optimized by heat emissions rather than the traditional metrics of energy use or utility costs. It will also be interesting to investigate how green building deisgn reduces heat emisssions compared with conventional buildings.

Acknowledgments

This research was supported by the Assistant Secretary for Energy Efficiency and Renewable Energy, Office of Building Technologies of the United States Department of Energy, under Contract No. DE-AC02-05CH11231, and by the European Union's Horizon 2020 research and innovation programme under grant agreement No. 691895 - project SHAR-LLM (Sharing Cities).

References

[1] C.M. Hsieh, T. Aramaki, K. Hanaki, Estimation of heat rejection based on the air conditioner use time and its mitigation from buildings in Taipei City, Build. Environ. 42 (2007) 3125–3137. doi:10.1016/j.buildenv.2006.07.029.

[2] K. Ward, S. Lauf, B. Kleinschmit, W. Endlicher, Heat waves and urban heat islands in Europe: A review of relevant drivers, Sci. Total Environ. 569–570 (2016) 527–539. doi:10.1016/j.scitotenv.2016.06.119.
[3] T.R. Oke, G. Mills, A. Christen, J.A. Voogt, Urban climates, Cambridge University Press, Cambridge, UK, 2017. doi:10.1016/s0168-6321(06)80036-2.
[4] G.J. Steeneveld, S. Koopmans, B.G. Heusinkveld, L.W.A. Van Hove, A.A.M. Holtslag, Quantifying urban heat island effects and human comfort for cities of variable size and urban morphology in the Netherlands, J. Geophys. Res. Atmos. 116 (2011) 1–14. doi:10.1029/2011JD015988.
[5] L. Kleerekoper, M. Van Esch, T.B. Salcedo, How to make a city climate-proof, addressing the urban heat island effect, Resour. Conserv. Recycl. 64 (2012) 30–38. doi:10.1016/j.resconrec.2011.06.004.
[6] C. Cao, X. Lee, S. Liu, N. Schultz, W. Xiao, M. Zhang, L. Zhao, Urban heat islands in China enhanced by haze pollution, Nat. Commun. 7 (2016) 1–7. doi:10.1038/ncomms12509.
[7] Z.S.M. Odli, I.A. Zakarya, F.N. Mohd, T.N.T. Izhar, N.M. Ibrahim, N. Mohamad, Green Roof Technology-Mitigate Urban Heat Island (UHI) Effect, MATEC Web Conf. 78 (2016). doi:10.1051/matecconf/20167801100.
[8] R.C. Grifoni, S. Tascini, E. Cesario, G.E. Marchesani, Cool façade optimization: A new parametric methodology for the urban heat island phenomenon (UHI), Conf. Proc. - 2017 17th IEEE Int. Conf. Environ. Electr. Eng. 2017 1st IEEE Ind. Commer. Power Syst. Eur. EEEIC / I CPS Eur. 2017. (2017) 1–5. doi:10.1109/EEEIC.2017.7977677.
[9] S. IPCC, M. Manning, Z. Chen, M. Marquis, K.B. Averyt, M. Tignor, H.L. Miller, IPCC Summary for policymakers, Clim. Chang. (2007).
[10] A. Salvati, M. Palme, G. Chiesa, M. Kolokotroni, Built form, urban climate and building energy modelling: case-studies in Rome and Antofagasta, J. Build. Perform. Simul. 0 (2020) 1–17. doi:10.1080/19401493.2019.1707876.
[11] M. Kolokotroni, Y. Zhang, R. Watkins, The London Heat Island and building cooling design, Sol. Energy. 81 (2007) 102–110. doi:10.1016/j.solener.2006.06.005.
[12] W. Köppen, Die Wärmezonen der Erde, nach der Dauer der heissen, gemässigten und kalten Zeit und nach der Wirkung der Wärme auf die organische Welt betrachtet (The thermal zones of the earth according to the duration of hot, moderate and cold periods and to the impac, Meteorol. Zeitschrift. 20 (1884) 351–360. doi:10.1127/0941-2948/2011/105.
[13] X. Yang, L.L.H. Peng, Z. Jiang, Y. Chen, L. Yao, Y. He, T. Xu, Impact of urban heat island on energy demand in buildings: Local climate zones in Nanjing, Appl. Energy. 260 (2020) 114279. doi:10.1016/j.apenergy.2019.114279.
[14] J. Schatz, C.J. Kucharik, Urban climate effects on extreme temperatures in Madison, Wisconsin, USA, Environ. Res. Lett. 10 (2015). doi:10.1088/1748-9326/10/9/094024.
[15] K.K. Roman, T. O'Brien, J.B. Alvey, O.J. Woo, Simulating the effects of cool roof and PCM (phase change materials) based roof to mitigate UHI (urban heat island) in prominent US cities, Energy. 96 (2016) 103–117. doi:10.1016/j.energy.2015.11.082.
[16] B. Pioppi, I. Pigliautile, C. Piselli, A.L. Pisello, Cultural heritage microclimate change: Human-centric approach to experimentally investigate intra-urban overheating and numerically assess foreseen future scenarios impact, Sci. Total Environ. 703 (2020) 134448. doi:10.1016/j.scitotenv.2019.134448.
[17] D.J. Sailor, A review of methods for estimating anthropogenic heat and moisture emissions in the urban environment, Int. J. Climatol. 31 (2011) 189–199. doi:10.1002/joc.2106.
[18] T. Hong, J. Yang, X. Luo, Heat Emissions from Buildings to Ambient Air, in: Proc. BS2019, Rome, Italy, 2019.
[19] A. Matzarakis, F. Rutz, H. Mayer, Modelling radiation fluxes in simple and complex environments - application of the RayMan model, Int. J. Biometeorol. 54 (2007) 131–139. doi:10.1007/s00484-009-0261-0.
[20] F. Lindberg, B. Holmer, S. Thorsson, SOLWEIG 1.0 - Modelling spatial variations of 3D radiant fluxes and mean radiant temperature in complex urban settings, Int. J. Biometeorol. 52 (2008) 697–713. doi:10.1007/s00484-008-0162-7.
[21] M. Bruse, Microclimate Simulations | ENVI_MET, (2011). https://www.envi-met.com/ (accessed October 22, 2018).
[22] J. Huang, J.G. Cedeño-Laurent, J.D. Spengler, CityComfort+: A simulation-based method for predicting mean radiant temperature in dense urban areas, Build. Environ. 80 (2014) 84–95. doi:10.1016/j.buildenv.2014.05.019.
[23] R. Harrison, B. McGoldrick, C.G.B. Williams, Artificial heat release from greater London, 1971-1976, Atmos. Environ. 18 (1984) 2291–2304. doi:10.1016/0004-6981(84)90001-5.
[24] D.J. Sailor, A. Brooks, Quantifying anthropogenic moisture emissions and their potential impact on the urban climate, in: American Meteorological Society (Ed.), 8th Symp. Urban Environ., American Meteorological Society, Phoenix, AZ, USA., 2009.
[25] R. Emmanuel, K. Steemers, Connecting the realms of urban form, density and microclimate, Build. Res. Inf. 46 (2018) 804–808. doi:10.1080/09613218.2018.1507078.
[26] S. Chatterjee, A. Khan, A. Dinda, S. Mithun, R. Khatun, H. Akbari, H. Kusaka, C. Mitra, S.S. Bhatti, Q. Van Doan, Y. Wang, Simulating micro-scale thermal interactions in different building environments for mitigating urban heat

islands, Sci. Total Environ. 663 (2019) 610–631. doi:10.1016/j.scitotenv.2019.01.299.
[27] S. Wonorahardjo, I.M. Sutjahja, Y. Mardiyati, H. Andoni, D. Thomas, R.A. Achsani, S. Steven, Characterising thermal behaviour of buildings and its effect on urban heat island in tropical areas, Int. J. Energy Environ. Eng. (2019). doi:10.1007/s40095-019-00317-0.
[28] A.L. Pisello, E. Fortunati, C. Fabiani, S. Mattioli, F. Dominici, L. Torre, L.F. Cabeza, F. Cotana, PCM for improving polyurethane-based cool roof membranes durability, Sol. Energy Mater. Sol. Cells. 160 (2017) 34–42. doi:10.1016/J.SOLMAT.2016.09.036.
[29] R. Sun, Y. Wang, L. Chen, A distributed model for quantifying temporal-spatial patterns of anthropogenic heat based on energy consumption, J. Clean. Prod. 170 (2018) 601–609. doi:10.1016/j.jclepro.2017.09.153.
[30] T. Ichinose, K. Hanaki, T. Matsuo, Analyses on Geographical Distribution of Urban Anthropogenic Heat Based on Very Precise Geographical Information, Environ. Eng. Res. 31 (1994) 263–273. doi:10.11532/proes1992.31.263.
[31] K.E. Torrance, J.S.W. Shun, Time-varying energy consumption as a factor in urban climate, Atmos. Environ. 10 (1976) 329–337. doi:10.1016/0004-6981(76)90174-8.
[32] F. Kimura, S. Takahashi, The effects of land-use and anthropogenic heating on the surface temperature in the Tokyo Metropolitan area: A numerical experiment, Atmos. Environ. Part B. Urban Atmos. 25 (1991) 155–164. doi:10.1016/0957-1272(91)90050-O.
[33] H. Taha, Modeling impacts of increased urban vegetation on ozone air quality in the South Coast Air Basin, Atmos. Environ. 30 (1996) 3423–3430. doi:10.1016/1352-2310(96)00035-0.
[34] K. Kłysik, Spatial and seasonal distribution of anthropogenic heat emissions in Lodz, Poland, Atmos. Environ. 30 (1996) 3397–3404. doi:10.1016/1352-2310(96)00043-X.
[35] S.-H. Lee, S.-T. Kim, Estimation of anthropogenic heat emission over South Korea using a statistical regression method, Asia-Pacific J. Atmos. Sci. 51 (2015) 157–166. doi:10.1007/s13143-015-0065-6.
[36] D. Sailor, M. Hart, An anthropogenic heating database for major U.S. cities, (2006).
[37] I.G. Hamilton, M. Davies, P. Steadman, A. Stone, I. Ridley, S. Evans, The significance of the anthropogenic heat emissions of London's buildings: A comparison against captured shortwave solar radiation, Build. Environ. 44 (2009) 807–817. doi:10.1016/j.buildenv.2008.05.024.
[38] B. Bueno, L. Norford, G. Pigeon, R. Britter, A resistance-capacitance network model for the analysis of the interactions between the energy performance of buildings and the urban climate, Build. Environ. 54 (2012) 116–125. doi:10.1016/j.buildenv.2012.01.023.
[39] U.S. Department of Energy, Commercial Reference Buildings, (n.d.). https://www.energy.gov/eere/buildings/commercial-reference-buildings.
[40] J. Yang, D. llamathy Mohan Kumar, A. Pyrgou, A. Chong, M. Santamouris, D. Kolokotsa, S.E. Lee, Green and cool roofs' urban heat island mitigation potential in tropical climate, Sol. Energy. 173 (2018) 597–609. doi:10.1016/j.solener.2018.08.006.
[41] I. Pigliautile, M. Chàfer, A.L. Pisello, G. Pérez, L.F. Cabeza, Inter-building assessment of urban heat island mitigation strategies: Field tests and numerical modelling in a simplified-geometry experimental set-up, Renew. Energy. 147 (2020) 1663–1675. doi:10.1016/j.renene.2019.09.082.
[42] B. Tremeac, P. Bousquet, C. de Munck, G. Pigeon, V. Masson, C. Marchadier, M. Merchat, P. Poeuf, F. Meunier, Influence of air conditioning management on heat island in Paris air street temperatures, Appl. Energy. 95 (2012) 102–110. doi:10.1016/j.apenergy.2012.02.015.
[43] S. Erba, A. Sangalli, L. Pagliano, Present and future potential of natural night ventilation in nZEBs, in: IOP Conf. Ser. Earth Environ. Sci., Institute of Physics Publishing, 2019. doi:10.1088/1755-1315/296/1/012041.
[44] U.S.D. of Energy, EnergyPlus Documentation Engineering Reference, 2019.
[45] U.S. Department of Energy, EnergyPlus™ Version 9.2.0 Documentation Engineering Reference, (2019) 1741. https://energyplus.net/documentation.
[46] U.S. Department of Energy's, EnergyPlus, (2018). https://energyplus.net/ (accessed December 20, 2018).
[47] L. Xuan, T. Hong, Modeling thermal interactions between buildings in urban context, in: Proc. BS2019, Rome, Italy, 2019.
[48] R. and A.-C.E. American Society of Heating, ANSI/ASHRAE Standard 140-2017 Standard Method Of Test For The Evaluation Of Building Energy Analysis Computer Programs, (2017).
[49] US-Doe, "Testing and validation" EnergyPlus Energy SImulation Software, (2014). http://apps1.eere.energy.gov/buildings/energyplus/energyplus_testing.cfm.
[50] American Society of Heating Refrigerating and Air-Conditioning Engineers, ANSI/ASHRAE 140 - Standard Method of Test for the Evaluation of Building Energy Analysis Computer Programs, (2011).
[51] M.C. Baechler, T.L. Gilbride, P.C. Cole, M.G. Hefty, K. Ruiz, Guide to Determining Climate Regions by County, Build. Technol. Off. - Build. Am. BEST Pract. Ser. 7.3 (2015).

https://www.energy.gov/sites/prod/files/2015/10/f27/ba_climate_region_guide_7.3.pdf.
[52] J.G. Powers, J.B. Klemp, W.C. Skamarock, C.A. Davis, J. Dudhia, D.O. Gill, J.L. Coen, D.J. Gochis, R. Ahmadov, S.E. Peckham, G.A. Grell, J. Michalakes, S. Trahan, S.G. Benjamin, C.R. Alexander, G.J. Dimego, W. Wang, C.S. Schwartz, G.S. Romine, Z. Liu, C. Snyder, F. Chen, M.J. Barlage, W. Yu, M.G. Duda, The Weather Research and Forecasting Model: Overview, System Efforts, and Future Directions, Bull. Am. Meteorol. Soc. 98 (2017) 1717–1737. doi:10.1175/BAMS-D-15-00308.1.
[53] A. Katal, M. Mortezazadeh, L. (Leon) Wang, Modeling building resilience against extreme weather by integrated CityFFD and CityBEM simulations, Appl. Energy. 250 (2019) 1402–1417. doi:https://doi.org/10.1016/j.apenergy.2019.04.192.